

ผลของขนาดเส้นผ่าศูนย์กลางท่อ ความดันภายนอกและการไหลด้วยโบรอน-ไนโตรเจนต่อ
โครงสร้างอิเล็กทรอนิกส์ของท่อนาโนคาร์บอนผนังเดี่ยว



นาย อาทิตย์ วงศ์อัจฉริยา

ศูนย์วิทยทรัพยากร
จุฬาลงกรณ์มหาวิทยาลัย

วิทยานิพนธ์นี้เป็นส่วนหนึ่งของการศึกษาตามหลักสูตรปริญญาวิทยาศาสตรมหาบัณฑิต

สาขาวิชาเคมี ภาควิชาเคมี

คณะวิทยาศาสตร์ จุฬาลงกรณ์มหาวิทยาลัย

ปีการศึกษา 2552

ลิขสิทธิ์ของจุฬาลงกรณ์มหาวิทยาลัย

EFFECTS OF TUBE DIAMETER, EXTERNAL PRESSURE AND BORON-NITROGEN
DOPING ON ELECTRONIC STRUCTURES OF SINGLE-WALLED CARBON
NANOTUBES



Mr. Arthit Vongachariya

ศูนย์วิทยทรัพยากร
จุฬาลงกรณ์มหาวิทยาลัย
A Thesis Submitted in Partial Fulfillment of the Requirements
for the Degree of Master of Science Program in Chemistry

Department of Chemistry

Faculty of Science

Chulalongkorn University

Academic Year 2009

Copyright of Chulalongkorn University

อาทิตย์ วงศ์อัจฉริยา : ผลของขนาดเส้นผ่านศูนย์กลางท่อ ความดันภายนอกและการโด๊ปด้วยโบรอน-ไนโตรเจนต่อโครงสร้างอิเล็กทรอนิกส์ของท่อนาโนคาร์บอนผนังเดี่ยว. (EFFECTS OF TUBE DIAMETER, EXTERNAL PRESSURE AND BORON-NITROGEN DOPING ON ELECTRONIC STRUCTURES OF SINGLE-WALLED CARBON NANOTUBES) อ. ที่ปรึกษาวิทยานิพนธ์หลัก : รศ.ดร. วุฒิชัย พาราสุข ,อ. ที่ปรึกษาวิทยานิพนธ์ร่วม: ผศ.ดร. ธิติ บวรรัตนารักษ์, 51 หน้า.

ได้ศึกษาโครงสร้างแถบอิเล็กทรอนิกส์ของท่อนาโนคาร์บอนแบบอาร์มแชร์และแบบซิกแซกที่มีขนาดเส้นผ่านศูนย์กลางท่อตั้งแต่ 3-10 Å โดยทฤษฎีเคอซีทีฟังก์ชันนัลกับเบสิสเซตเชิงตัวเลข ระยะเงื่อนไขขอบถูกนำมาใช้ในการคำนวณทั้งหมด พบว่าสมบัติทางอิเล็กทรอนิกส์ขึ้นกับไครลเวกเตอร์ และเส้นผ่านศูนย์กลางท่อ ความสัมพันธ์ระหว่างช่องว่างแถบพลังงานกับเส้นผ่านศูนย์กลางแสดงให้เห็นจุดสูงสุดที่เส้นผ่านศูนย์กลางท่อค่าหนึ่งๆ และช่องว่างแถบพลังงานจะเข้าสู่ค่าๆหนึ่งที่เส้นผ่านศูนย์กลางขนาดใหญ่ ช่องว่างแถบพลังงานของ (3i+1) และ (3i+2) ของท่อนาโนคาร์บอนแบบซิกแซกดูเหมือนจะเข้าสู่ค่าเดียวกันที่เส้นผ่านศูนย์กลางท่อขนาดใหญ่โดยช่องว่างแถบพลังงานของท่อนาโนคาร์บอนแบบซิกแซกแปรผกผันกับเส้นผ่านศูนย์กลางท่อ ส่วนท่อนาโนคาร์บอนแบบอาร์มแชร์แปรผกผันกับเส้นผ่านศูนย์กลางกำลังสอง แบบจำลองท่อนาโนคาร์บอนแบบซิกแซก (8,0) และอาร์มแชร์ (5,5) ได้ถูกใช้ในการศึกษาผลของการโด๊ปด้วยโบรอนและไนโตรเจน โครงสร้างแถบพลังงานของท่อนาโนคาร์บอนแบบซิกแซกเปลี่ยนแปลงตามตำแหน่งการโด๊ปด้วยโบรอนและไนโตรเจนตามระนาบ XY เท่านั้น ในขณะที่โครงสร้างแถบพลังงานของท่อนาโนคาร์บอนแบบอาร์มแชร์ขึ้นทั้งกับระนาบ XY และ Z ตำแหน่งที่เหมาะสมในการโด๊ปด้วยโบรอนและไนโตรเจนคือตำแหน่งที่มีระยะระหว่างโบรอนและไนโตรเจนอะตอมสั้นที่สุดและมีสปินอิเล็กทรอนิกส์แบบซิงเกิลต งานวิจัยชิ้นนี้ยังทำการคำนวณโครงสร้างแถบพลังงานของท่อนาโนคาร์บอนแบบซิกแซก (8,0) และอาร์มแชร์ (5,5) ที่ไม่ได้โด๊ปและโด๊ปด้วยโบรอนและไนโตรเจนอะตอมที่สภาวะอัตราส่วนความเครียดต่างๆ เพื่อทำการศึกษาอิทธิพลของความดันภายนอกที่มีต่อท่อนาโนคาร์บอน พบค่าช่องว่างแถบพลังงานเปลี่ยนไปตามอัตราส่วนความเครียดต่างๆ การโด๊ปด้วยโบรอนและไนโตรเจนเกือบไม่มีผลต่อค่ามอดูลัสของยัง และยังคงมีค่าอยู่ในระดับ TPa สำหรับท่อนาโนคาร์บอนแบบซิกแซกความดันภายนอกที่มีค่าอัตราส่วนความเครียดทั้งที่เป็นบวกและลบจะไปลดค่าช่องว่างแถบพลังงาน ในขณะที่แม้ว่าเห็นผลกระทบของความดันภายนอกแต่ก็ไม่พบรูปแบบที่ชัดเจนสำหรับท่อนาโนคาร์บอนแบบอาร์มแชร์ ผลของการศึกษานี้สามารถนำไปประยุกต์ในการเลือกท่อนาโนคาร์บอนได้อย่างเหมาะสม อันเป็นประโยชน์ต่องานประยุกต์ในอุปกรณ์อิเล็กทรอนิกส์

ภาควิชา.....เคมี..... ลายมือชื่อนิติศ.....อาทิตย์ วงศ์อัจฉริยา.....
 สาขาวิชา.....เคมี..... ลายมือชื่อ อ.ที่ปรึกษาวิทยานิพนธ์หลัก.....
 ปีการศึกษา...2552..... ลายมือชื่อ อ.ที่ปรึกษาวิทยานิพนธ์ร่วม.....

5172554723 : MAJOR CHEMISTRY

KEYWORDS : DFT / CARBON NANOTUBES

ARTHIT VONGACHARIYA : EFFECTS OF TUBE DIAMETER, EXTERNAL PRESSURE AND BORON-NITROGEN DOPING ON ELECTRONIC STRUCTURES OF SINGLE-WALLED CARBON NANOTUBES. THESIS ADVISOR : ASSOC. PROF. VUDHICHAI PARASUK, Ph.D., THESIS CO-ADVISOR : ASST. PROF. THITI BOVORNANARAKS, Ph.D., 51 pp.

Electronic band structures of zigzag and armchair single-walled carbon nanotube (SWCNT) with tube diameter from 3-10 Å were investigated by density function theory with numerical basis set. The periodic boundary condition was implemented for all calculations. The electronic properties depend on chiral vectors and tube diameters. The dependence of SWCNTs band gap energy on tube diameters shows the maximum at certain tube diameter. The band gap energy converges to a particular values at large diameter. Band gap energies of $(3i+1)$ and $(3i+2)$ zigzag SWCNTs seems to converge to the same values at large diameter. Their band gap energies vary inversely with tube diameter, whereas those of armchair SWCNT vary inversely with $(\text{tube diameter})^2$. Zigzag (8,0) and armchair (5,5) SWCNTs were used to investigate the effect of boron and nitrogen (B-N) doping. The electronic band structures of B-N doped SWCNTs change with the position of doping only on the XY plane for zigzag SWCNTs while it depends on both of XY plane and Z axis for armchair SWCNTs. The favorable B-N doping position on SWCNTs is that with the smallest B-N distance in singlet spin state. Electronic band structures of undoped and B-N doped zigzag (8,0) and armchair (5,5) SWCNT were also calculated at various strain ratio (ϵ) to investigate the effect of external pressure. The change in band gap energies at various strain conditions has been observed. The B-N doping has almost no effect on Young's modulus, and its magnitude remains in the order of TPa. For zigzag SWCNTs, external pressure with both positive and negative strain ratios could reduce its band gap energy whereas no regular patterns are observed for armchair SWCNTs. This understanding could be applied for selection of appropriate SWCNTs which could be useful for electronic devices application.

Department : _____ Chemistry _____	Student's Signature _____ <i>Arthit Vongachariya</i>
Field of Study : _____ Chemistry _____	Advisor's Signature _____ <i>Vudhichai Parasuk</i>
Academic Year : _____ 2009 _____	Co-Advisor's Signature _____ <i>Thiti Bovornanarak</i>

ACKNOWLEDGEMENTS

I would like to express my deep gratitude to a number of people who give me the guidance, help and support to accomplish my study. First of all, I would like to give all gratitude affectionately to my parents for all support and encouragement during the whole period of my study

I also would like to express my sincere gratitude to Associate Professor Dr. Vudhichai Parasuk, my advisor, for his multifarious understanding, useful guidance, kind suggestion and encouragement throughout my study, especially patience during the time of this thesis preparation. This is also to my co-advisor Assistant Professor Dr. Thiti Bovornratanaraks. Again, I am grateful thanks to Assistant Professor Dr. Warinthorn Chavasiri, Associate Professor Dr. Mongkol Sukwattanasinitt and Assistant Professor Dr. Yuthana Tantirungrotechai who are my thesis committee.

Finally, I would like to acknowledge the Computational Chemistry Unit Cell (CCUC), Department of Chemistry, Faculty of Science, Chulalongkorn University for computer resource and other facilities. I also would like acknowledge the financial support by the 90th of Chulalongkorn University Fund (Ratchadaphiseksomphot Endowment Fund) of Chulalongkorn University and National Center of Excellence for Petroleum, Petrochemicals, and Advanced Materials, NCE-PPAM.

ศูนย์วิทยทรัพยากร
จุฬาลงกรณ์มหาวิทยาลัย

CONTENTS

	Page
ABSTRACT IN THAI.....	iv
ABSTRACT IN ENGLISH.....	v
ACKNOWLEDGEMENTS.....	vi
CONTENTS.....	vii
LIST OF TABLES.....	ix
LIST OF FIGURES.....	x
CHAPTER I INTRODUCTION	
1.1 History of carbon nanotube (CNT).....	1
1.2 Structural and Chiral Vector of Carbon nanotube.....	1
1.3 Electronic Properties of Carbon Nanotube.....	4
1.4 Objective of the Present Study.....	6
CHAPTER II THEORY	
2.1 Quantum Mechanics.....	7
2.2 Spatial Orbital and Spin Orbital.....	9
2.3 Hartree-Fock Approximation.....	10
2.4 Density Functional Theory.....	12
2.5 Basis Sets.....	14
2.6 Periodic Calculations.....	15
CHAPTER III COMPUTATIONAL DETAILS	
3.1 Effect of Tube Diameter.....	18
3.2 Effect of B-N Doping.....	19
3.3 Effect of External Pressure.....	20
CHAPTER IV RESULT AND DISCUSSIONS	
4.1 Effect of Tube Diameter and Chiral Vector.....	22
4.2 Effect of B-N Doping.....	30

4.3 Effect of External Pressure.....	40
CHAPTER V CONCLUSION.....	37
REFERENCES.....	39
VITAE.....	40



ศูนย์วิทยทรัพยากร
จุฬาลงกรณ์มหาวิทยาลัย

LIST OF TABLES

Table		Page
3.1	Strain ratio and c unit cell parameter on SWCNT structures.....	21
4.1	Numbers of HOMO and LUMO lobes per number of carbon hexagonal ring on one empirical cell and patterns.....	28
4.2	Spin densities on boron atom and nitrogen atom of zigzag (8,0) SWCNTs.....	32
4.3	Spin densities on boron atom and nitrogen atom of armchair (5,5) SWCNTs.....	33
4.4	Young's modulus value obtained from DFT comparing with other calculation and experimental works.....	41



ศูนย์วิทยทรัพยากร
จุฬาลงกรณ์มหาวิทยาลัย

Figure		
1.1	Structural displays of a) SWCNT and b) MWCNT.....	2
1.2	The direction of wrapping defined by two directional vector R_1 and R_2 on the graphene sheet.....	3
1.3	The structures of a) zigzag b) armchair and c) chiral SWCNT.....	3
3.1	Structures in PBC of a) zigzag SWCNT and b) armchair SWCNT.....	18
3.2	Structures of BN-doped a) zigzag SWCNT and b) armchair SWCNT.....	20
4.1	Strain energy per carbon atom of SWCNTs optimized structure as a function of a) tube diameter and b) reverse square diameter.....	23
4.2	Band gap energy of SWCNTs optimized structure with varying tube diameter.....	24
4.3	Relation between band gap energy a) and $1/D$, where D is the tube diameter of zigzag $n=3i+1$ and $n=3i+2$ SWCNTs in the range of 3-21 Å b) and $1/D^2$, where D is the tube diameter of armchair SWCNTs in the range of 5-19 Å *the metallic SWCNTs show zero energy band gap.....	25
4.4	Bond Distance and Bond angle of zigzag SWCNTs on various diameters.....	27
4.5	HOMO and LUMO of $n=3i+2$ zigzag SWCNTs.....	25
4.6	Relative energies for the B-N doping as a function of B-N distance of B-N doped a) zigzag (8,0) and b) armchair (5,5) SWCNTs.....	31
4.7	Charge on doped atom in a) zigzag (8,0) and b) armchair (5,5) SWCNTs as functions of position of doping , In the inset solid line represent charge on boron atom and dash line represent charge on nitrogen atom.....	35
4.8	Correlation between relative energies and B-N distance reciprocal consideration by symmetry of doping a) odd number and b) even number on round direction of B-N doping for zigzag SWCNT.....	36
4.9	Calculated band structure of a) undoped zigzag (8,0) SWCNT b) B-N	38

Figure

	doped zigzag (8,0) SWCNT at 1a position of doping c) undoped armchair (5,5) SWCNT and d) B-N doped armchair (5,5) SWCNT at 0b position of doping.	
4.10	Band gap energy (E_g) of undoped and B-N doped a) zigzag (8,0) b) armchair (5,5) SWCNT as a function of doping position.....	39
4.11	Relative energy of undoped and B-N doped zigzag (8,0) and armchair (5,5) SWCNT as a function of strain ratio.....	40
4.11	Band gap energy (E_g) of undoped and B-N doped a) zigzag (8,0) and b) armchair (5,5) SWCNT as a function of strain ratio.....	43



ศูนย์วิทยทรัพยากร
จุฬาลงกรณ์มหาวิทยาลัย

CHAPTER I

INTRODUCTION

1.1 History of Carbon Nanotube (CNT)

The first time that the world explore carbon nanotube is not certainty but many group believe that carbon nanotube might have used to contribute the strength of steel in the middle ages, roughly 5th to 15th century. In 1952 Radushkevich and Lukyanovich reported hollow graphitic carbon tubular form nature that are 50 nanometers in diameter in Journal of Physical Chemistry of Russia. However, the access to Russian publications was not easy in the period of the cold war and Russian language was no encouraging thus, this finding was not listed in databases^{1,2}. In 1976 the hollow carbon fiber with nanometer scale diameter synthesized by chemical vapor deposition technique was shown by Oberlin, Endo and Koyama³. In 1979 carbon nanotube synthesized on carbon anode in arc discharge was presented at the 14th Biennial Conference for Carbon at Pennsylvania State University by Abrahamsom⁴ as carbon fibers and it was characterized and hypothesized for their growth at low pressures in nitrogen atmosphere. The popular literature attributes the discovery of CNT synthesized by arc discharge was presented by Iijima⁵ in 1991. After that, due to their excellent physical, chemical, mechanical and electronic properties, carbon nanotube are being the most studied carbon-based nanomaterial.

1.2 Structural and chiral vector of Carbon Nanotube

Carbon nanotube is an allotrope of carbon with its shape like a cylindrical tube of carbon atoms in the quasi-one dimensional structure. It can be categorized as single-walled carbon nanotubes (SWCNTs) and multi-walled carbon nanotube (MWCNTs) as shown in Figure 1.1. The SWCNT structure can be conceptualized by Hamada notation which is the wrapping of a carbon sp^2 layer called graphene sheet into the cylindrical shape. The wrapped direction is mostly represented by a pair of indices

(n,m) called the chiral vector⁶ as illustrated in figure 1.2. The integer n and m refer to the size of vectors along two directions defined by unit vectors R_1 and R_2 in the graphene sheet. If $n=m$, the SWCNT are called armchair. If $m=0$, the SWCNT are called zigzag. Otherwise are called chiral as shown in figure 1.3.

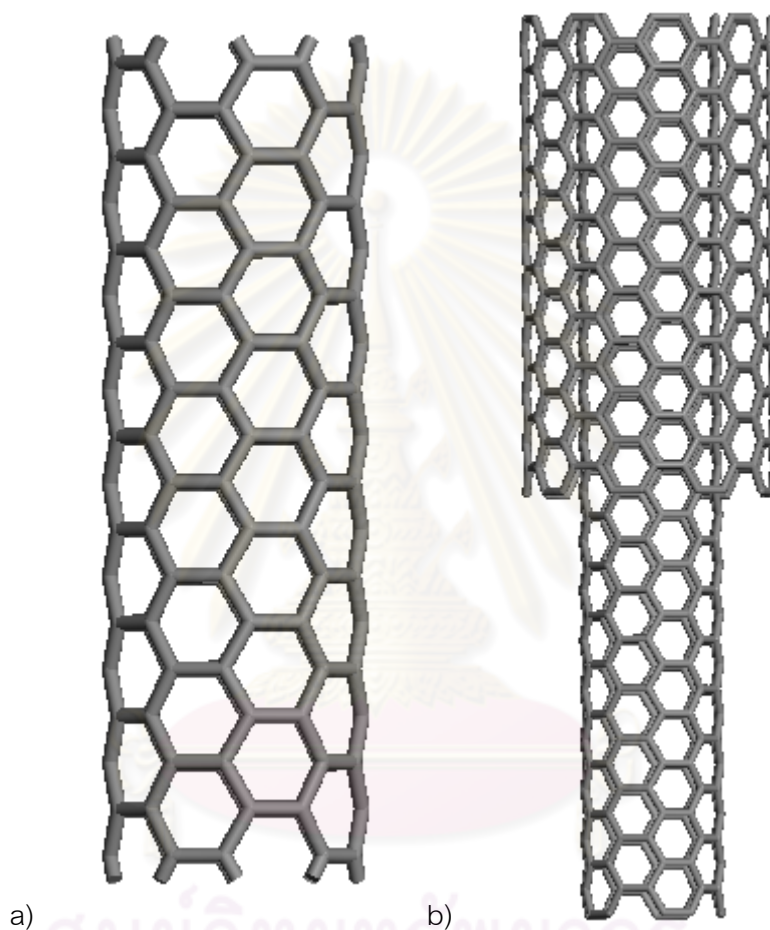


Figure 1.1 structural displays of a) SWCNT and b) MWCNT

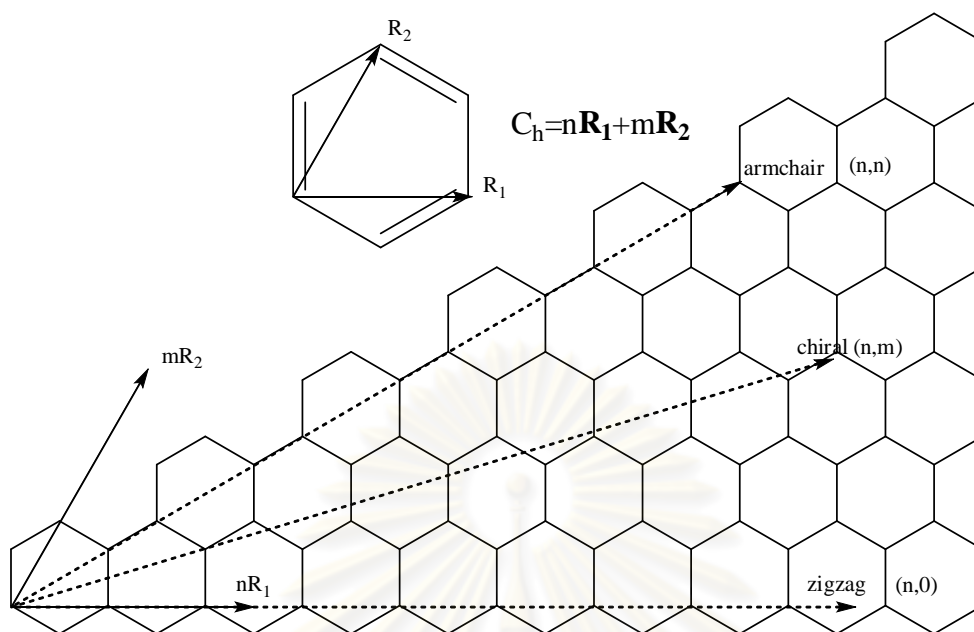


Figure 1.2 The direction of wrapping defined by two directional vector R_1 and R_2 on the graphene sheet

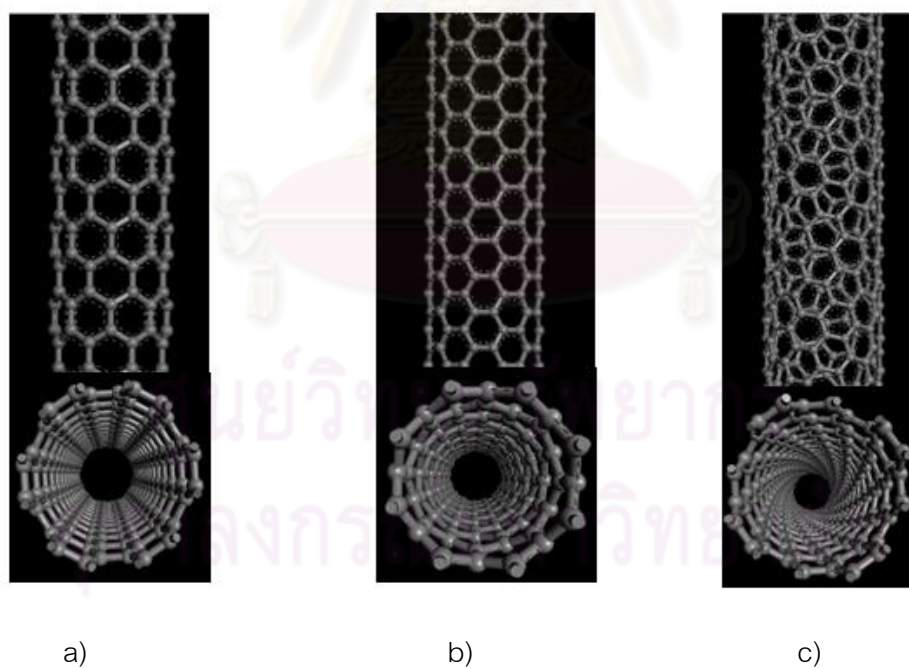


Figure 1.3 The structures of a) zigzag b) armchair and c) chiral SWCNT

1.3 Electronic Properties of Carbon Nanotube

The potential applications of carbon nanotube are enormous. Major applications often take advantage of their unique electronic properties. The uniqueness on electronic properties of SWCNT is directly related to their structures. It is generally accepted that SWCNTs with $(n-m)/3 = \text{integer}$ are metallic otherwise they are semiconductor⁷. All armchair ($n=m$) and zigzag with n being a multiple of 3 carbon nanotubes are metallic, and other zigzag carbon nanotube are semiconductor. This is known as the 1/3 rule performed by zone folding approximation (ZF)^{7, 8}. The band gap energy of semiconductor zigzag SWCNTs was found to decrease inversely with tube diameter and chiral vector by ZF prediction. This result is in agreement with the Hartree-Fock approximation⁹. However, the reliability of ZF as well as the HF method for predicting the band gap energy is often questioned. Recently, while the density functional theory (DFT)^{10, 11} calculations revealed zigzag SWCNTs ($n,0$) with $n=3-5$ to be metallic, HF and ZF predicted them to be insulator and semiconductor, respectively. Due to the σ - π hybridization effect¹¹ becomes more important with decreasing tube diameter. However, the σ - π hybridization effect can increase the steric repulsion inside the tube such that smaller diameter tubes are energetically less favorable than larger tubes. Previously, growing of SWCNT with very small diameter was produced inside zeolite channels¹² and multi-walled nanotubes¹³. It shows that the energetic effect of small diameter nanotube can be modified if taken in to account¹⁴ the steric repulsion inside the channel.

An effective and efficient way to modify the electronic properties of semiconductor is by heteroatom substitution. For CNTs, substitution of carbon atoms by boron or nitrogen atoms has been the most-studied at the level of experimentals¹⁵⁻²³ and theoreticals²⁴⁻²⁷. It is found that the band gap energy and Fermi energy level of doped SWCNTs can be controlled by dopant atom. However, the most of theoretical calculations did not investigate the electron spin of doped SWCNTs system except the work of Owens et al.²⁸. They investigated electron spin and magnetic properties of boron or nitrogen doped SWCNTs by using HF theory with cluster model of doped SWCNTs.

Their result revealed that the most favorable configuration, the high spin electronic state in boron or nitrogen doped zigzag SWCNT, has been observed. However, the representation of SWCNTs by the cluster model is questionable. Doping of both boron and nitrogen atoms represent a promising approach for modifying the electronic properties of CNTs as a function of their chemical composition. However, boron nitride nanotube are semiconductors with a constant gap of 5.8 eV⁹ without depending on their geometries whereas it is well known that undoped SWCNTs present a metallic and semiconductor behavior with depending on their geometry (chiral vector). Recently, the synthesis of B-N doped SWCNTs was reported by using chemical vapor deposition²⁹, laser ablation¹⁶ and arc discharge¹⁵. It is shown that B-N doping in SWCNTs can decrease the band gap energy. Moradian and Azadi³⁰ investigated the B-N doped zigzag (10,0) SWCNTs by using DFT calculation of average quantities contribution of each configuration of doping. They found that band gap energy of the B-N doped SWCNTs can be controlled by the concentration dopant. However, the effect of B-N doping position is still questioned.

Another important fascinating property of CNT is a high mechanical strength related to be 100 times stronger than steel^{9, 31-33}. Thus, it is a promising material for device under high pressure conditions. However, few investigations on electronic properties of SWCNTs under external pressure have been performed under various strains^{9, 34-36}. The results indicate the significant dependent of the tube strain on the band gap energy. Normally, these strains can be induced by chemical treatment, electric and magnetic fields, and mechanical means. However, to our knowledge the investigation on electronic properties under external pressure of B-N doped SWCNTs has not yet been reported.

1.4 Objective of the Present Study

on the objective of this work is to investigate the uniqueness of electronic and properties and mechanical properties of SWCNTs by using density functional theory calculation. Specifically, we aim to:

- I. Study effect of tube diameter and chiral vector on electronic structure of SWCNTs,
- II. Study effect of boron and nitrogen doping on electronic structure of SWCNTs,
- III. Study effect of external pressure on electronic structure of undoped and B-N doped SWCNTs, and
- IV. Study the mechanical properties of undoped and B-N doped SWCNTs



CHAPTER II

THEORY

2.1. Quantum Mechanics

Before the twentieth century, objects can be described as the rigid body particles with mass " m ". Their properties could be calculated according to classical mechanics such as

$$\text{Kinetic energy} = \frac{1}{2}mv^2 \quad (2.1)$$

$$\text{Force} = \frac{dp}{dt} = \frac{d(mv)}{dt} = ma \quad (2.2)$$

where v is the velocity of the object

p is the momentum of the object

t is the time progresses

Later, it became clear that classical mechanics alone were incapable of explaining several phenomena especially for very small objects such as electrons and other subatomic particles. These limitations of the classical mechanics led to a revolution in scientific principles, and quantum mechanics (QM) has then been developed in the early decades of the 20th century.

Quantum mechanics is an accepted scientific principle which describes the behavior of small particles in atomic and subatomic scales. Schrödinger equation or wave mechanic is per se the usual formulation for solving quantum mechanical problems or chemical problems. This equation is based on the concept of wave-particle duality, all matter exhibits both wave-like and particle-like properties. According to Louis de Broglie³⁷, the particle wavelength, λ , which is a wave-like property of a particle is related to its linear momentum, p

$$p = \frac{h}{\lambda} \quad (2.3)$$

where h is Plank's constant.

Hence, following this concept and the mathematical description of the differential equation for the standing wave, Erwin Schrödinger proposed famous equation that bears his name

$$\left(-\frac{\hbar^2}{8\pi^2m}\nabla^2 + \hat{V}\right)\Psi = E\Psi. \quad (2.4)$$

Here Ψ is the wavefunction, \hat{V} is the potential operator, E is the system energy, and ∇ is the differential operator.

In abbreviation, the equation is written as

$$\hat{H}\Psi = E\Psi \quad (2.5)$$

when

$$\hat{H} = \hat{T} + \hat{V} \quad (2.6)$$

where \hat{H} is the Hamiltonian and \hat{T} is the kinetic operator.

In mathematics, an equation of this form is called an eigen-value equation. Ψ is called the eigenfunction and E is an eigenvalue. According to Heisenberg, the operator and eigenfunction can be represented as matrix or vectors, respectively.

In quantum chemistry, the wavefunction Ψ is a function of the electron and nuclei positions. The square of this function is a probabilistic description of electron and nuclei behavior. As such, it can describe the probability of electrons and nuclei being in certain locations, but it cannot give exact locations of the particles. The wavefunction is also called a probabilities amplitude. In order to obtain a physically relevant solution of the Schrödinger equation, the wave function must be continuous, single-valued, normalizable and antisymmetric with respect to the interchange of fermion particles. The total Hamiltonian operator can be written in terms of the kinetic and potential operators of nuclei and electrons.

$$\hat{H}_{tot} = \hat{T}_n + \hat{T}_e + \hat{V}_{ne} + \hat{V}_{ee} + \hat{V}_{nn} \quad (2.7)$$

where \hat{T}_n is the kinetic operator of nuclei, \hat{T}_e is the kinetic operator of electrons, \hat{V}_{ne} is the potential operator representing electron-nuclei attraction, \hat{V}_{ee} is the

potential operator representing electron-electron repulsion, and \hat{V}_{nn} is the potential operator representing nucleus-nucleus repulsion.

With such complexly Hamiltonian, solving the Schrödinger equation exactly is impossible. To reduce the complexation, the Hamiltonian operator can be separated into two parts to a good approximation, where one part describes the electronic motion and another part describes nuclear motion. This approximation is called Born-Oppenheimer approximation. It is convenient to decouple these two motions, and compute electronic energy for fixed nuclear positions. The nuclear kinetic energy term is taken to be independent of the electrons, correlation in the attractive electron-nuclear potential energy term is eliminated and the repulsive nuclear-nuclear potential energy term becomes a simply evaluate constant for a given geometry. Hence, the electronic Hamiltonian is taken to be

$$\hat{H}_{el} = \hat{T}_e + \hat{V}_{ne} + \hat{V}_{ee} \quad (2.8)$$

and the electronic Schrödinger equation is

$$\hat{H}_{el}\Psi_{el}(\mathbf{q}_i, \mathbf{q}_k) = E_{el}\Psi_{el}(\mathbf{q}_i, \mathbf{q}_k) \quad (2.9)$$

where subscript 'el' emphasizes the invocation of the Born-Oppenheimer approximation and \mathbf{q}_i is the electronic coordinate and the \mathbf{q}_k is the nuclear coordinate which is treated as parameter. The eigenvalue of the electronic Schrödinger equation is the electronic energy. If the electronic Schrödinger equation is solved, the nuclear Schrödinger equation can also be solved with electronic energy being the potential term. However, the Schrödinger equations for electronic system can exactly be solved only for the one electron system. Methods of approximation have been developed for solving the Schrödinger equations for many-electron systems.

2.2 Spatial Orbital and spin orbitals.

An orbital has been defined as a one-electron wavefunction. A spatial orbital $\varphi_i(\mathbf{r})$ is a function of the position vector \mathbf{r} and give details of an electron spatial distribution such that $|\varphi_i(\mathbf{r})|^2 d\mathbf{r}$ is the probability of finding an electron in the small

proximity $d\mathbf{r}$ surrounding \mathbf{r} . To have such meaning, a set of spatial orbital satisfies the orthonormal condition.

$$\int d\mathbf{r} \varphi_i^*(\mathbf{r})\varphi_j(\mathbf{r}) = \delta_{ij} \quad (2.10)$$

If the set of spatial orbitals $\{\varphi_i(\mathbf{r})\}$ were complete, then any arbitrary function $f(\mathbf{r})$ could be exactly expanded as

$$f(\mathbf{r}) = \sum_{i=1}^{\infty} a_i \varphi_i(\mathbf{r}) \quad (2.11)$$

The wavefunction for an electron that describes both its spatial distribution and spin is the spin orbital, $\chi(\mathbf{x})$, where \mathbf{x} indicates both spatial and spin coordinates.

$$\chi(\mathbf{x}) = \begin{cases} \varphi(\mathbf{r})\alpha(\omega) \\ \text{or} \\ \varphi(\mathbf{r})\beta(\omega) \end{cases} \quad (2.12)$$

2.3 Hartree-Fock approximation

Since the orbital model is a very attractive one, and it is clear to be used successfully as the model for atom, molecule and solid state. The Hartree-Fock approximation (HF) solves the electronic Schrödinger equation for many-electron systems by assuming a single electron moves in the potential that averages out the effects of the nuclei and the remaining electrons. Electron repulsion is certainly not taken to be zero, but the HF approximation cannot treat the finer details of electronic structure theory that are caused by the instantaneous repulsion between electrons.

The HF approximation defines the ground state of N-many-electron wavefunction by Slater determinant.

$$\Psi = \frac{1}{\sqrt{(N)!}} \begin{vmatrix} \chi_1(1) & \chi_2(1) & \chi_3(1) & \cdots & \chi_N(1) \\ \chi_1(2) & \chi_2(2) & \chi_3(2) & \cdots & \chi_N(2) \\ \chi_1(3) & \chi_2(3) & \chi_3(3) & \cdots & \chi_N(3) \\ \vdots & \vdots & \vdots & \ddots & \vdots \\ \chi_1(N) & \chi_2(N) & \chi_3(N) & \cdots & \chi_N(N) \end{vmatrix} \quad (2.13)$$

or in case of restricted closed-shell Hartree-Fock (RHF) where $N = 2n$

$$\Psi = \frac{1}{\sqrt{(2n)!}} \begin{vmatrix} \varphi_1(1)\alpha(1) & \varphi_1(1)\beta(1) & \varphi_2(1)\alpha(1) & \cdots \\ \varphi_1(2)\alpha(2) & \varphi_1(2)\beta(2) & \varphi_2(2)\alpha(2) & \cdots \\ \varphi_1(3)\alpha(3) & \varphi_1(3)\beta(3) & \varphi_2(3)\alpha(3) & \cdots \\ \vdots & \vdots & \vdots & \cdots \\ \varphi_1(2n)\alpha(2n) & \varphi_1(2n)\beta(2n) & \varphi_2(2n)\alpha(2n) & \cdots \end{vmatrix} \dots \quad (2.14)$$

where $\frac{1}{\sqrt{(2n)!}}$ is the normalization constant

Although there is no exact analytical solution to the Schrödinger equation for system that contains more than one electron, the standard numerical techniques can achieve approximate solutions. The usual approach in quantum chemistry is to build the total wavefunction from the linear combination of a set of orthogonal functions called 'basis function'. In practice, the basis set is referred to a set of atomic orbitals, so this approach is called 'Linear Combination of Atomic Orbital to form Molecular Orbital (LCAO-MO)'. Thus, the molecular orbital i (φ_i) can be built from k atomic orbitals (ϕ_k)

$$\varphi_i = \sum_{\mu=1}^{\kappa} c_{\mu i} \phi_{\mu} \quad (2.15)$$

where $c_{\mu i}$ is the molecular coefficient.

Form an approach which constructs a determinantal wavefunction from a set of LCAO-MOs, what it remains is to verify the MO coefficients ($c_{\mu i}$). This could be achieved by optimizing the molecular wavefunction for a particular system with the variation method. The procedure would guarantee that the energy eigenvalue is always an upperbound to the exact energy. Thus, the lowest energy from the minimized set of molecular coefficients will give the best approximation to the exact wavefunction for the chosen basis set.

The variational constraint leads to a set of algebraic equations (Roothaan-Hall)^{38, 39} for $c_{\mu i}$ expressed in matrix form as

$$\mathbf{FC} = \mathbf{SC}\epsilon \quad (2.16)$$

where \mathbf{C} is the matrix of MO coefficient, \mathbf{F} the Fock matrix which is the sum of a term representing the energy of a single electron in the field of the bare atomic nuclear and a term describing electron-electron repulsion within an averaged field of

electron density, \mathbf{S} is the matrix which describing the overlap of molecular orbitals and $\mathbf{\epsilon}$ is the diagonal matrix containing the energies of each orbital.

Since the terms within the Fock matrix \mathbf{F} depend upon the electron density, which in turn, depends upon molecular wavefunction defined by the matrix of MO coefficients \mathbf{C} . The Roothan-Hall equation is nonlinear and must be solved by an iterative method so, it is called 'self-consistent field' (SCF) method. Leading to convergence of the SCF method, the minimum-energy MOs produce the electric field which generates the same orbitals (hence, the self-consistency).

However, each electron in HF approximation moves in an average field of other electron and nuclear thus, this approximation neglects electron correlation that can lead to the large deviation from exact values.

2.4 Density functional theory

Density functional theory (DFT) is a method to investigate the electronic structure. In this theory, the properties of system are considered by using functionals of electron density. Thus, this method is called density functional theory. The DFT reduces the dimension of the electronic structure theory drastically. The only problem left is that the universal functional connecting to the electron density are still unknown. DFT is very popular for calculations of solid state physics since 1970s because its results for solid state systems agreed well with experiment data in many cases. Now, DFT is the most popular method for investigation of electronic structures in chemistry and physics. However, the main problems for recent functionals of DFT are the inability to systematically improve them and the poor description of van der Waals interactions.

Density functional theory was proven by the two Hohenberg-Kohn theorems⁴⁰. The first theorem expresses that the ground state properties of a N-electron system are uniquely defined by the ground state electron density (ρ). Thus, the ground state energy (E_0) is the functional of ρ , written as $E_0 = E_0[\rho]$. However, this theorem did not propose the means to obtain the exact ρ .

The second Hohenberg-Kohn theorem proves that the energy functional of the trial ground state density, $\tilde{\rho}$, is an upperbound to the exact energy, E_0 .

$$E_{trial}[\tilde{\rho}] \geq E_0[\rho] \quad (2.17)$$

However, this theorem still was not proposed to compute the energy from the trial electron density.

In 1965, Kohn and Sham⁴¹ suggested an idea to calculate the ground state energy based on the N-electron non-interacting system. For this system, the ground state energy can be expressed as

$$\begin{aligned} E[\rho] &= T_s[\rho] + V_{ne}[\rho] + J[\rho] + E_{xc}[\rho] \quad (2.18) \\ &= -\frac{1}{2} \sum_{i=0}^n \langle \varphi_i | \nabla^2 | \varphi_i \rangle + \sum_{\alpha} \int \frac{Z_{\alpha} \rho(1)}{|r_{1\alpha}|} d\vec{r} + \frac{1}{2} \iint \frac{\rho(1)\rho(2)}{r_{12}} d\vec{r}_1 d\vec{r}_2 + E_{xc}[\rho] \end{aligned}$$

where φ_i is Kohn-Sham orbital, $T_s[\rho]$ is the kinetic energy functional for independent electron, $V_{ne}[\rho]$ is the electron-nuclear attraction functional or external potential, $J[\rho]$ is the coulomb interaction functional and $E_{xc}[\rho]$ is the exchange-correlation energy functional. $\rho(1)$ can be expressed as

$$\rho = \sum_{i=1}^n |\varphi_i|^2 \quad (2.19)$$

The final term in equation 2.18, the exchange-correlation energy functional, is the only term that is still unknown. The first simple and good approximation is to assume that the density is a slowly varying function. It means that the density is local and can be treated as a uniform electron gas. For LDA, the exchange-correlation energy functional ($E_{xc}[\rho]$) can be written as

$$E_{xc}^{LDA}[\rho] = \int \rho(r) \varepsilon_{xc}(\rho(r)) dr \quad (2.20)$$

where $\varepsilon_{xc}(\rho(r))$ is the exchange-correlation energy per particle of a uniform electron gas of density $\rho(r)$. This term can be split in to exchange (ε_x) and correlation (ε_c) contributions.

$$\varepsilon_{xc}(\rho(r)) = \varepsilon_x(\rho(r)) + \varepsilon_c(\rho(r)) \quad (2.21)$$

The exchange functional part is first given by Dirac formula and has been developed by Slater⁴² (S) in 1972. The correlation functional part, which is purely dynamical correlation, has been parameterized from the quantum Monte Carlo results by Vosko, Wilk and Nusair⁴³ (VWN). This approximation can be extended to the unrestricted open shell system and it is called the “local spin-density approximation” or LSDA.

$$E_{xc}^{LSDA}[\rho_\alpha\rho_\beta] = \int \rho(r)\varepsilon_{xc}(\rho_\alpha(r),\rho_\beta(r))dr \quad (2.22)$$

To improve over the LSDA approach, the non-uniform electron gas must be considered. The first derivative of the electron density has been included to the exchange and correlation functionals. Such the approach is known as the “Generalized Gradient Approximation” (GGA) or non-local approximation.

$$E_{xc}^{GGA}[\rho_\alpha\rho_\beta] = \int \rho(r)\varepsilon_{xc}(\rho_\alpha(r),\rho_\beta(r),\nabla\rho_\alpha(r),\nabla\rho_\beta(r))dr \quad (2.23)$$

Using GGA, improved results for molecular geometries and ground-state energies are obtained. In particular, the most widely used GGA functional for the solid state system is the Perdew-Burke-Ernzerhof⁴⁴ (PBE) exchange-correlation functional, a direct GGA parameterization, because it can give reasonable bond length and good lattice constants in bulk solid⁴⁵. Although DFT results are usually accurate for most systems, there is no systematically way for improving these functionals. Thus, the current DFT approach can not estimate the error of the calculation without comparing to other methods or experimental results.

2.5 Basis sets

The basis set is the set of orthogonal functions used for construction of molecular orbitals. These functions usually are functions which used for described atomic orbitals for atomic and molecular system, therefore they center on atoms. The atomic orbitals are Slater type orbitals that decayed exponentially with distance from the nucleus. However, the overlap and 2-electron integrals with Slater-type orbitals are difficult to calculate analytically. Therefore, Gaussian-type orbitals that lead to simpler integrals and reduced computational costs were preferred instead. Another alternative is

the basis function which gives numerical values on an atomic-centered spherical-polar mesh. This type of basis set is called "numerical basis set". For the numerical basis set^{46, 47}, the radial part is obtained by solving the atomic DFT equations numerically. In addition, a reasonable level of accuracy is usually obtained by using about 300 radial points from the nucleus to an outer distance of 10 Bohr. A set of cubic spline for each of the 300 sections are stored radial functions thus, the radial part is piecewise analytic. The use of the exact DFT spherical atomic orbitals has several advantages. The molecule can be dissociated exactly to its constituent atoms. The basis set superposition effects has been minimized. Therefore, it can give the excellent results even for weak bonds.

The most simple of the molecular orbitals operate only one basis function for each atomic orbital up to the valence orbitals. These basis set is minimal basis set. Conversely, the minimal basis set still cannot describe well in most cases since, the exponent has only one value. This effect lead to an inability to explain differently charge distribution on atom and the size of orbital cannot be changed in the different environment. To increase the flexibility, the basis set is decontracted. When two or more basis functions are used to describe each atomic orbital, the basis set is called the extended basis set. In the split-valence basis set, two functions (or more) are required for description of the atomic orbital in the valence space, while orbitals for inner core electrons are treated with single function. Examples of the split-valence basis set are SVP, 6-31G and DN basis sets.^{46, 47} Nevertheless, the extended basis set still give the unsophisticated results in the case of high polar or high strain systems. Since, the flexibility on the shape of orbitals is needed to be included. The higher angular momentum functions are added to increase the flexibility of the orbitals. This expansion is called polarization function. For example, DN basis set is added with single d function on all non-hydrogen atoms and DND basis set is formed. DNP basis set is expanded from DND by including a p function on hydrogen atom.

2.6 Periodic calculations

A fundamental unit cell being repeated to form an infinite system can be used to describe the periodic system. Not only periodicity can be extended in three dimensions as in solid state system but also be in one or two dimensions as in polymer and surface systems. The three dimensions unit cell can be considered with lattice unit vector \mathbf{a}_i where $i = 1, 2$ and 3 spanning the physical space, with length and the angles between them defining the shape. For the simplest cell, it could take $\mathbf{a}_1 = (1,0,0)$; $\mathbf{a}_2 = (0,1,0)$ and $\mathbf{a}_3 = (0,0,1)$. The periodic system can be generated by translation of the unit cell.

The periodicity of the centered atoms in the system requires that the wavefunction and the electron density must display the same periodicity. The Bloch theorem is used to describe the periodicity. It states that the wavefunctions at equivalent positions in different cell are related by a complex phase factor connecting the lattice vector \mathbf{R} and \mathbf{a} vector in the reciprocal space.

$$\phi(\mathbf{r} + \mathbf{R}) = e^{i\mathbf{k}\cdot\mathbf{R}}\phi(\mathbf{r}) \quad (2.24)$$

where vector \mathbf{r} describe a point in real space while vector \mathbf{k} describe a point in reciprocal space.

The Bloch theorem expresses the crystalline orbital (ϕ) for the n th band in the unit cell and can be written as a wave-like part and cell-periodic part (φ) called a Bloch orbital

$$\phi_{n,\mathbf{k}}(\mathbf{r}) = e^{i\mathbf{k}\cdot\mathbf{R}}\varphi_n(\mathbf{r}) \quad (2.25)$$

The Bloch orbital can be expanded into a set of nuclear-centered basis function (χ_j).

$$\phi_{n,\mathbf{k}}(\mathbf{r}) = \sum_j^m \sum_R c_{nj} e^{i\mathbf{k}\cdot\mathbf{R}} \chi_j(\mathbf{r} + \mathbf{R}) \quad (2.26)$$

Now, the system has been transformed to an infinite number of orbitals in only treating within unit cell. The solutions become a function of the reciprocal space

vector \mathbf{k} within the first Brillouin zone. Hence matrix equation of the variation problem has been formulated to equation 2.27

$$\mathbf{F}^{\mathbf{k}}\mathbf{C}^{\mathbf{k}} = \mathbf{S}^{\mathbf{k}}\mathbf{C}^{\mathbf{k}}\epsilon^{\mathbf{k}} \quad (2.27)$$

The solutions are continuous as a function of \mathbf{k} , and provide a range of energies called a band energy. Total energy per unit cell can be calculated by integrating over \mathbf{k} space. As the principle in molecular system, the equivalent of the highest occupied molecular orbital (HOMO) is the Fermi energy level. The energy different between the top of the highest filled band and the bottom of the lowest empty band is called band gap. It is equivalent to HOMO-LUMO gap in molecular system. The systems with a zero band gap are metallic. Those with a non-zero band gap are insulator or semiconductor. It is depending on size of the gap compared with the thermal energy kT .



ศูนย์วิทยทรัพยากร
จุฬาลงกรณ์มหาวิทยาลัย

CHAPTER III

COMPUTATIONAL DETAILS

3.1 Effect of Tube Diameter

Structures of zigzag (n,0) and armchair (m,m) single-walled carbon nanotubes (SWCNT), where n being 4-26 and m being 4-14 with tube diameter from 3-20 Å were generated by the Material Studio 4.3 program. The periodic boundary condition⁴⁸ (PBC) was implemented. The 1x1x2 and 1x1x3 supercells were employed for zigzag and armchair SWCNTs, respectively, as shown in Figure 3.1. The carbon nanotubes were placed in a tetragonal cell with following cell constants, $\alpha = \beta = 90^\circ$ and $\gamma = 120^\circ$. Structure and cell volume optimizations and energies were carried out using density functional calculations based on generalized gradient approximation (GGA) with Perdew, Burke and Ernzerhof⁴⁴ (PBE) exchange-correlation functional with Dmol3 package. For basis set, double numerical basis set plus d polarization function (DND) was used^{46, 47}. Density of state and orbital analysis were carried out within the first Brillouin zone. The k-point sampling was made 4 k points along the tube and gamma points within the Monkhost-Pack scheme⁴⁹.

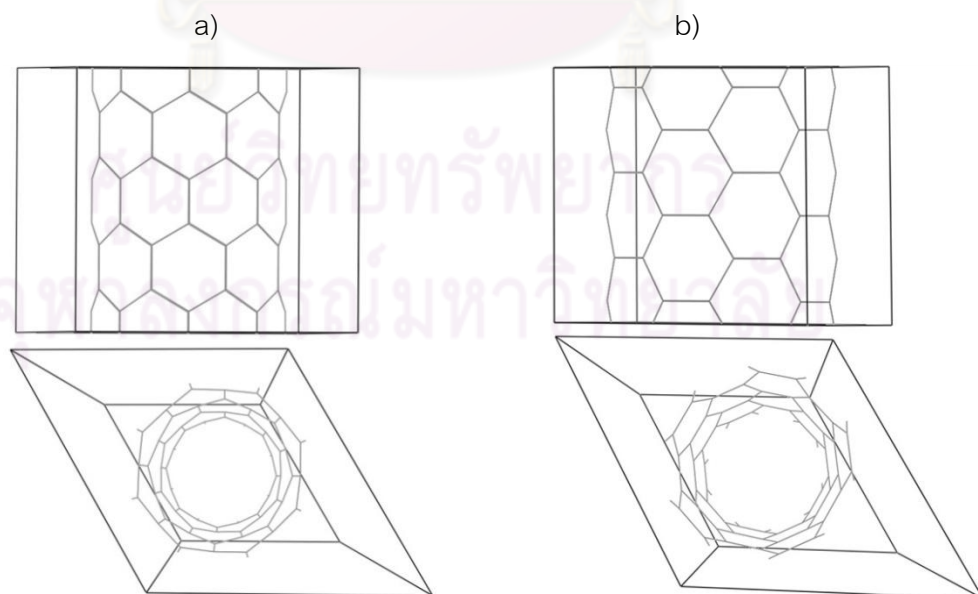


Figure 3.1 Structures in PBC of a) zigzag SWCNT and b) armchair SWCNT

3.2 Effect of B-N Doping

Two pairs of boron and nitrogen atoms have been substituted on carbon atoms in zigzag (8,0) and armchair (5,5) SWCNT to control the dopant concentration at approximately 3% to simulate experimental concentration. The B-N doping position were varied to investigate possible doping sites. The boron atoms were defined as the reference position. The substitution of nitrogen atoms perimeter circumference was done in two directions, i.e period and round directions, as shown in figure 3.2. The round position starts from 0-8 and 0-9 for zigzag and armchair, respectively. The position zero refers to the Boron reference. The period direction starts from a-d for all models. a being the Boron reference. All B-N doped SWCNT structures were generated with the Material Studio 4.3 program in the periodic boundary conditions (PBC). The 3 spin states i.e. singlet, triplet and quintet were considered. Geometry optimizations were performed using density functional calculations based on generalized gradient approximation (GGA) with Perdew, Burke and Ernzerhof (PBE) exchange-correlation function on Dmol3 package. Double numerical basis set plus d and p polarization function (DNP) was used. Zigzag (8,0) and armchair (5,5) SWCNT model has been described in tetragonal lattice where the cell parameters are $\alpha = \beta = 90^\circ$, $\gamma = 120^\circ$, $a=b=20 \text{ \AA}$ and $c = 17.07$ and 14.80 \AA with four times (128 atoms) and six times (120 atoms) supercell respectively. A 4 k-point Monkhorst-Pack grid along the tube axis has been used for Brillouin zone integration.

ศูนย์วิทยทรัพยากร
จุฬาลงกรณ์มหาวิทยาลัย

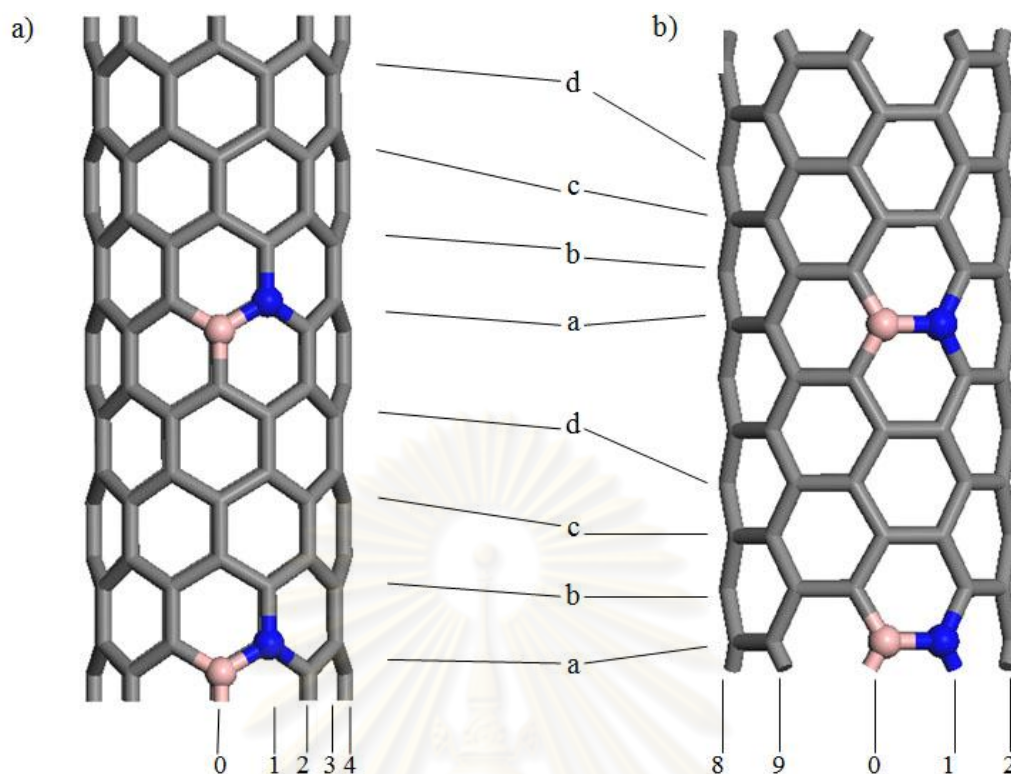


Figure 3.2 Structures of BN-doped a) zigzag SWCNT and b) armchair SWCNT

3.3 Effect of External Pressure

Undoped and the most stable isomer form of B-N doped (8,0) zigzag and (5,5) armchair SWCNT were selected for investigations. Various strain ratio (ϵ) from -0.1 to 0.1 were employed. Table 3.1 displayed the strain ratio with c cell parameter. Geometry optimizations were performed using density functional calculations based on generalized gradient approximation (GGA) with Perdew, Burke and Ernzerhof (PBE) functional and DNP basis set on Dmol³ package. The models have been described in tetragonal lattice where the cell parameters are $\alpha = \beta = 90^\circ$, $\gamma = 120^\circ$, $a=b=20$ with various c parameter matched with strain ratio as shown in table 3.1. A 4 k sampling point in Brillouin zone with Monkhorst-Pack grid along the tube axis has been used for calculation.

Table 3.1 Strain ratio and c unit cell parameter on SWCNT structures

(8,0) SWCNT		(8,0) Doped SWCNT		(5,5) SWCNT		(5,5) Doped SWCNT	
ϵ	c	ϵ	c	ϵ	c	ϵ	c
-0.10	15.36	-0.10	15.38	-0.10	13.31	-0.10	13.33
-0.09	15.53	-0.09	15.55	-0.09	13.46	-0.09	13.48
-0.08	15.70	-0.08	15.72	-0.08	13.61	-0.08	13.63
-0.07	15.88	-0.07	15.89	-0.07	13.75	-0.07	13.77
-0.06	16.05	-0.06	16.06	-0.06	13.90	-0.06	13.92
-0.05	16.22	-0.05	16.24	-0.05	14.05	-0.05	14.07
-0.04	16.39	-0.04	16.41	-0.04	14.20	-0.04	14.22
-0.03	16.56	-0.03	16.58	-0.03	14.35	-0.03	14.37
-0.02	16.73	-0.02	16.75	-0.02	14.49	-0.02	14.51
-0.01	16.90	-0.01	16.92	-0.01	14.64	-0.01	14.66
0.00	17.07	0.00	17.09	0.00	14.79	0.00	14.81
0.01	17.24	0.01	17.26	0.01	14.94	0.01	14.96
0.02	17.41	0.02	17.43	0.02	15.09	0.02	15.11
0.03	17.58	0.03	17.60	0.03	15.23	0.03	15.25
0.04	17.75	0.04	17.77	0.04	15.38	0.04	15.40
0.05	17.92	0.05	17.94	0.05	15.53	0.05	15.55
0.06	18.09	0.06	18.12	0.06	15.68	0.06	15.70
0.07	18.26	0.07	18.29	0.07	15.83	0.07	15.85
0.08	18.44	0.08	18.46	0.08	15.97	0.08	15.99
0.09	18.61	0.09	18.63	0.09	16.12	0.09	16.14
0.10	18.78	0.10	18.80	0.10	16.27	0.10	16.29

CHAPTER IV

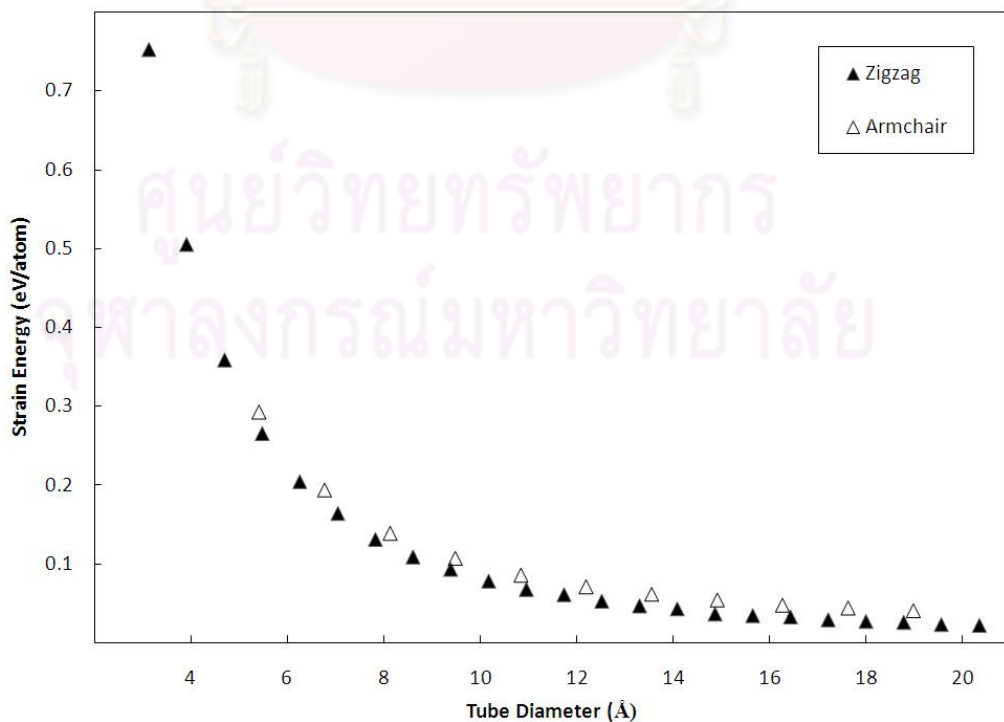
RESULTS AND DISCUSSIONS

4.1 Effect of Tube Diameter and Chiral Vector

The strain energy per atom (relative to graphene sheet) of SWCNT was determined according to

$$E_{strain} = E_{SWCNTs/atom} - E_{graphene/atom} \quad (4.1)$$

The values were then plotted with tube diameters in the range of 3 to 21 Å for armchair and zigzag SWCNTs and shown in Figure 4.1a. As the tube diameter decreasing, SWCNT rapidly becomes more unstable. The strain energies of both armchair and zigzag SWCNTs also show linear relationship with respect to square of the tube diameter ($1/D^2$) as displayed in Figure 4.1b. This observation agrees well with previous theoretical study⁹. It is worth to note that for similar tube diameters armchair SWCNTs have higher strain energy than the zigzag structures as evident by the higher value of slope in Figure 4.1b.



a)

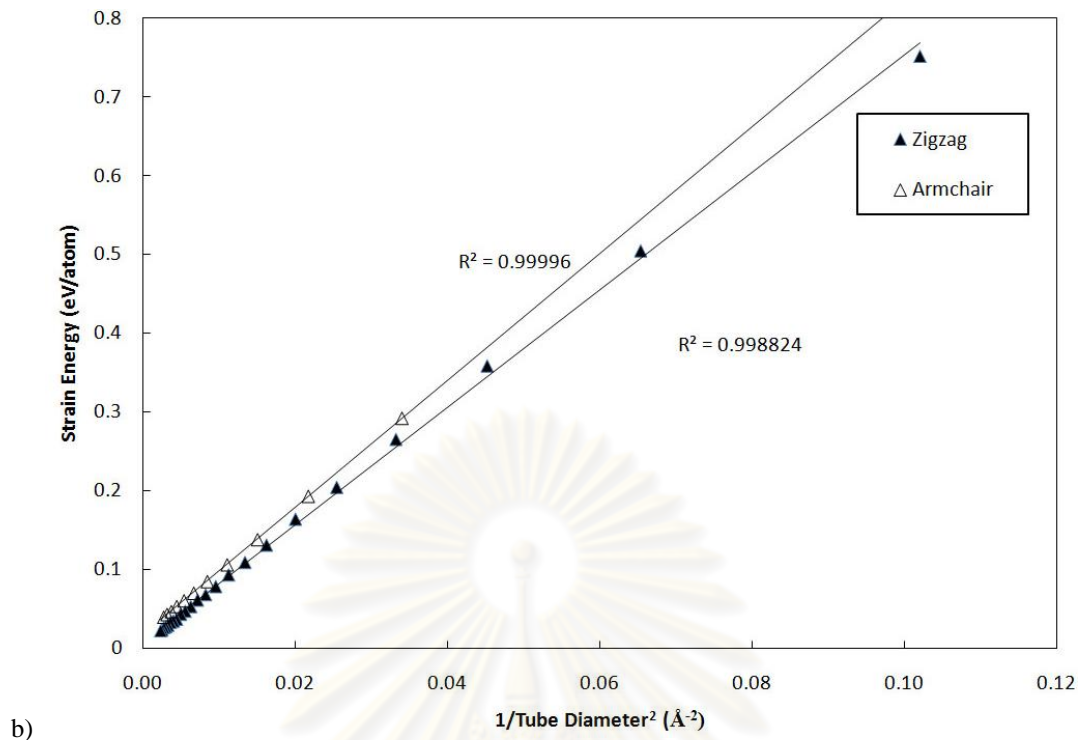


Figure 4.1 Strain energy per carbon atom of SWCNTs optimized structure as a function of a) tube diameter and b) reverse square diameter

The diameter and the chiral vector of carbon nanotube are interrelated and they can represent each other. To investigate the effect of tube diameter as well as chiral vector on electronic properties of zigzag and armchair SWCNTs, the band gap energies of relaxed SWCNTs at various tube diameters were determined using PBE/DND and the results were illustrated in Figure 4.2. Three types of zigzag SWCNTs, i.e. $n=3i$, $n=3i+1$ and $n=3i+2$, were investigated. The plot between band gap energies (E_g) and tube diameters for armchair and zigzag SWCNTs shows a maximum at a certain tube diameter. All type of SWCNTs with the smallest tube diameter ($< 5 \text{ \AA}$) are found to be metallic or semimetal ($< 7 \text{ \AA}$) with very small E_g (less than 0.6 eV). The metallic property of very small diameter SWCNTs has never been observed when using zone folding scheme (ZF)⁸ and tight-binding based method^{50, 51} as well as the Hartree-Fock approximation^{9, 10}. However, it was observed when using DFT calculations^{10, 11}. The small band gap was suggested to be the result of the σ - π hybridization in carbon atoms¹¹. The curve for (3i)-zigzag SWCNT has the maximum E_g of 0.1 eV at the diameter of 7 \AA . Thus, (3i)-zigzag SWCNT shows metallic or semi-metal property for all diameter-

range. For the armchair SWCNT, the maximum E_g of 0.45 eV is also observed at the diameter of 7 Å. The band gap energy for armchair SWCNT drops gradually after the maximum and reaches the value of 0.1 eV at the diameter of 16 Å. Although, with the maximum being noticed the armchair SWCNT maintains the metallic property at all tube diameter. The curves for (3i+1)- and (3i+2)-zigzag SWCNT show the maxima at 8 (0.75 eV) and 9 Å (0.9 eV), respectively. Their band gap energies converge to the value of 0.0 eV, they could become metal, at very large diameter.

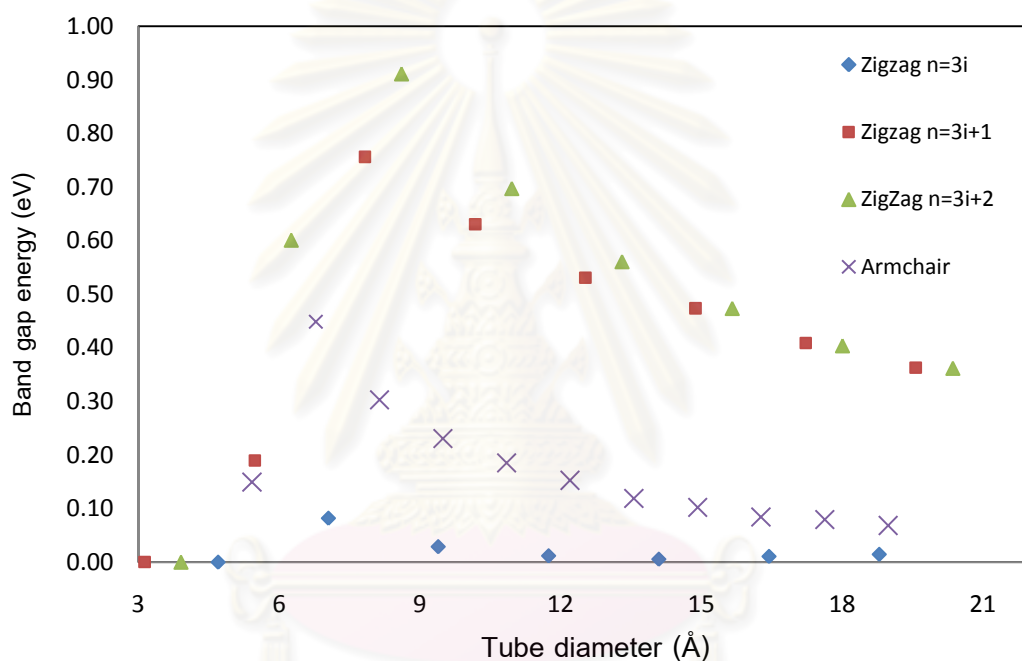


Figure 4.2 Band gap energy of SWCNTs optimized structures varying with tube diameters

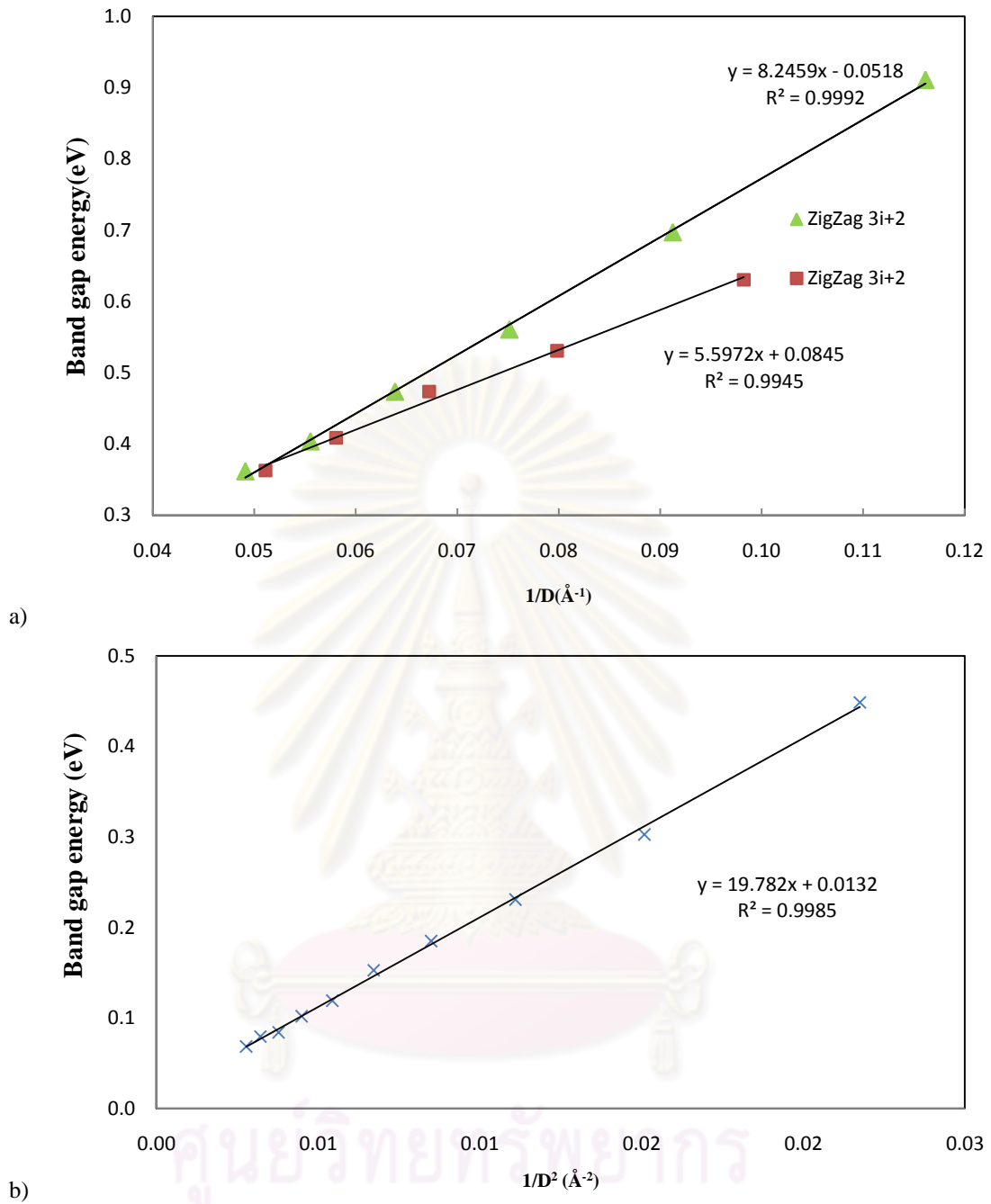


Figure 4.3 Relation between band gap energy a) and $1/D$, where D is the tube diameter of zigzag $n=3i+1$ and $n=3i+2$ SWCNTs in the range of 3-21 Å b) and $1/D^2$, where D is the tube diameter of armchair SWCNTs in the range of 5-19 Å *the metallic SWCNTs show zero band gap energy

Clearly, all $(3i+1)$ - and $(3i+2)$ -zigzag SWCNTs with the diameter larger than 8 Å are semi-conductor. Interestingly, both $(3i+1)$ - and $(3i+2)$ -zigzag SWCNTs converge to the same value of band gap energy of 0.0 eV at large tube diameter.

Moreover, energies band gap for (3i+1)- and (3i+2)-zigzag SWCNTs show linear dependencies with $1/D$ where D being tube diameter as displayed in Figure 4.3a. Although band gaps of both (3i+1)- and (3i+2)-zigzag SWCNT are linear to $1/D$, they do not share the same slope. However, a linear relationship with $1/D^2$ which was found for armchair SWCNT (Figure 4.3b). These results allow us to predict the trends for electronic properties (conductivity) of SWCNT in relation to the tube diameters. The distinct features of armchair and zigzag SWCNTs display different natures of their electronic properties. The $1/D$ and $1/D^2$ dependences also hint the influence of the external potential to the electronic energy of SWCNT.

In Figure 4.4, dependencies of bond distances ($B1$ and $B2$) and bond angles ($A1$ and $A2$) of zigzag SWCNTs with various tube diameters are displayed. The $B1$ and $B2$ parameters represent bond distances along tube axis (c direction) and circumference (ab plane), respectively, while $A1$ and $A2$ represent the $B1/B2$ and $B2/\text{neighboring } B2(B2')$ bond angles, respectively. From the plot, it is observed that while $B1$ increases exponentially, $B2$ decreases in the similar manner with tube diameters and both values converge to 1.425 \AA (carbon-carbon graphitic bond length). For the bond angle, $A1$ holds constant at 120° for almost entire range of SWCNT diameters whereas $A2$ is 107.5° for (4,0) SWCNT and raises with tube diameters to the value of 120° . The value of 120° implies the sp^2 hybridization whereas the angle of 107.5° represents the sp^3 hybridization for carbon atom. The change in bond lengths and bond angles shows rapid deviation from sp^2 to sp^3 hybridization when tube diameter is smaller than 7 \AA . This is in accordance with Figure 4.1a where the abrupt shift of the strain energy before 7 \AA being observed. It also confirms the strong σ - π effect for smallest tube diameter and in agreement with the deviations of band gap energy in Figure 4.2.

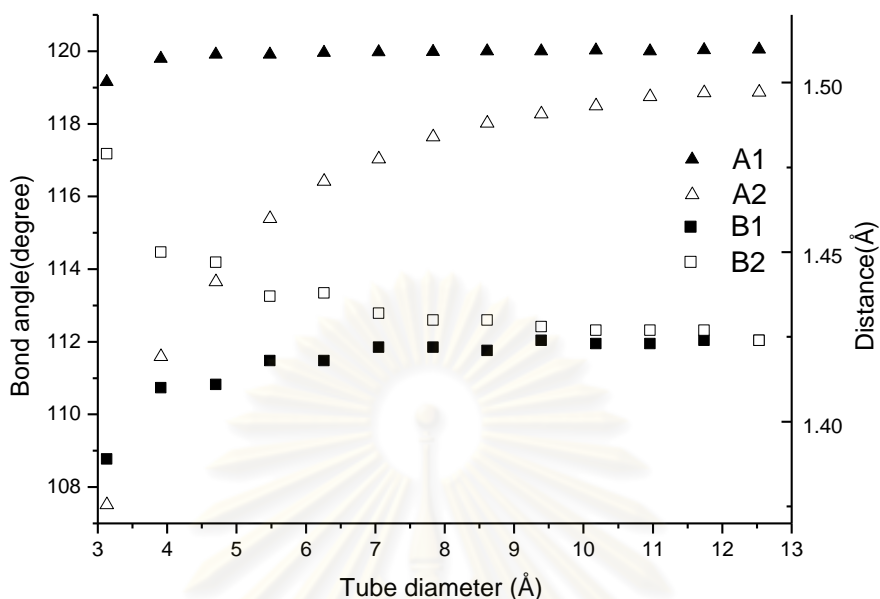


Figure 4.4 Bond Distance and Bond angle of zigzag SWCNTs on various tube diameters

To understand electronic properties of SWCNT, orbital analysis were applied for HOMO and LUMO of these compounds. For $(3i+2)$ -zigzag SWCNTs, plots of their HOMOs and LUMOs when $n = 5, 8, 11, 14,$ and 17 were generated and shown in Figure 4.5. The result indicated that HOMOs and LUMOs of zigzag SWCNT with $n = 11, 14$ and 17 have similar shape and pattern but they differ from those with $n = 5$ and 8 . For HOMOs and LUMOs, the patterns of numbers of lobes on B1 and B2 bonds per numbers of hexagonal rings are given in Table 3.1. These patterns are distinct for different SWCNTs and can also reflect the behavior in Figure 4.2. The patterns are $2i/3i/3i$ and $0/2i/3i$ for HOMO and LUMO for $(3i)$ -zigzag SWCNT except for $(3,0)$ zigzag. The patterns for $(3i+1)$ -zigzag SWCNT are $0/2i/3i+1$ and $2i+2/2(i-1)/3i+1$ for HOMO and LUMO at large tube diameters and $3i+1/2i/3i+1$ and $3i+1/2i/3i+1$ at small tube diameters. Also, the HOMO and LUMO patterns for $(3i+2)$ -zigzag are $4i+2/2(i-1)/3i+2$ and $0/2i+2/3i+2$ at large diameter and $4i+2/2i/3i+2$ and $4i+2/4i/3i+2$ at small diameter. For armchair SWCNT, the HOMO and LUMO patterns become n/n and $2n/n$. These results are in agreement with the band gap energy tendency shown in Figure 2. We observed that at very small tube diameter ($<7 \text{ \AA}$) patterns for HOMO or LUMO of

SWCNTs deviate from large tube diameter ($>7 \text{ \AA}$). This deviation is in agreement with the observation on the strain energy.

Table 4.1 Numbers of HOMO's and LUMO's lobes per number of carbon hexagonal ring on one empirical cell and patterns

Type	(n,m)	No. lobes on B1 / B2 /No. C rings		Patterns	
		HOMO	LUMO	HOMO	LUMO
Zigzag/n=3i	(6,0)	4/6/6	4/0/6	2i/3i/3i	2i/0/3i
	(9,0)	6/9/9	0/6/9	2i/3i/3i	0/2i/3i
	(12,0)	8/12/12	0/8/12	2i/3i/3i	0/2i/3i
	(15,0)	10/15/15	0/10/15	2i/3i/3i	0/2i/3i
	(18,0)	12/15/15	0/12/18	2i/3i/3i	0/2i/3i
Zigzag/n=3i+1	(4,0)	4/2/4	4/2/4	3i+1/2i/3i+1	3i+1/2i/3i+1
	(7,0)	0/4/7	7/0/7	0/2i/3i+1	3i+1/0/3i+1
	(10,0)	0/6/10	8/6/10	0/2i/3i+1	2i+2/2i/3i+1
	(13,0)	0/8/13	10/6/13	0/2i/3i+1	2i+2/2(i-1)/3i+1
	(16,0)	0/10/16	12/8/16	0/2i/3i+1	2i+2/2(i-1)/3i+1
Zigzag/n=3i+2	(5,0)	6/2/5	6/4/5	4i+2/2i/3i+2	4i+2/4i/3i+2
	(8,0)	10/2/8	8/0/8	4i+2/2(i-1)/3i+2	3i+2/0/3i+2
	(11,0)	14/4/11	0/8/11	4i+2/2(i-1)/3i+2	0/2i+2/3i+2
	(14,0)	18/6/14	0/10/14	4i+2/2(i-1)/3i+2	0/2i+2/3i+2
	(17,0)	22/8/17	0/12/17	4i+2/2(i-1)/3i+2	0/2i+2/3i+2
Armchair n=m	(4,4)	4/4	8/4	n/n	2n/n
	(5,5)	5/5	10/5	n/n	2n/n
	(6,6)	6/6	12/6	n/n	2n/n
Graphite		4/3	4/3	-	-

ศูนย์วิทยทรัพยากร
จุฬาลงกรณ์มหาวิทยาลัย

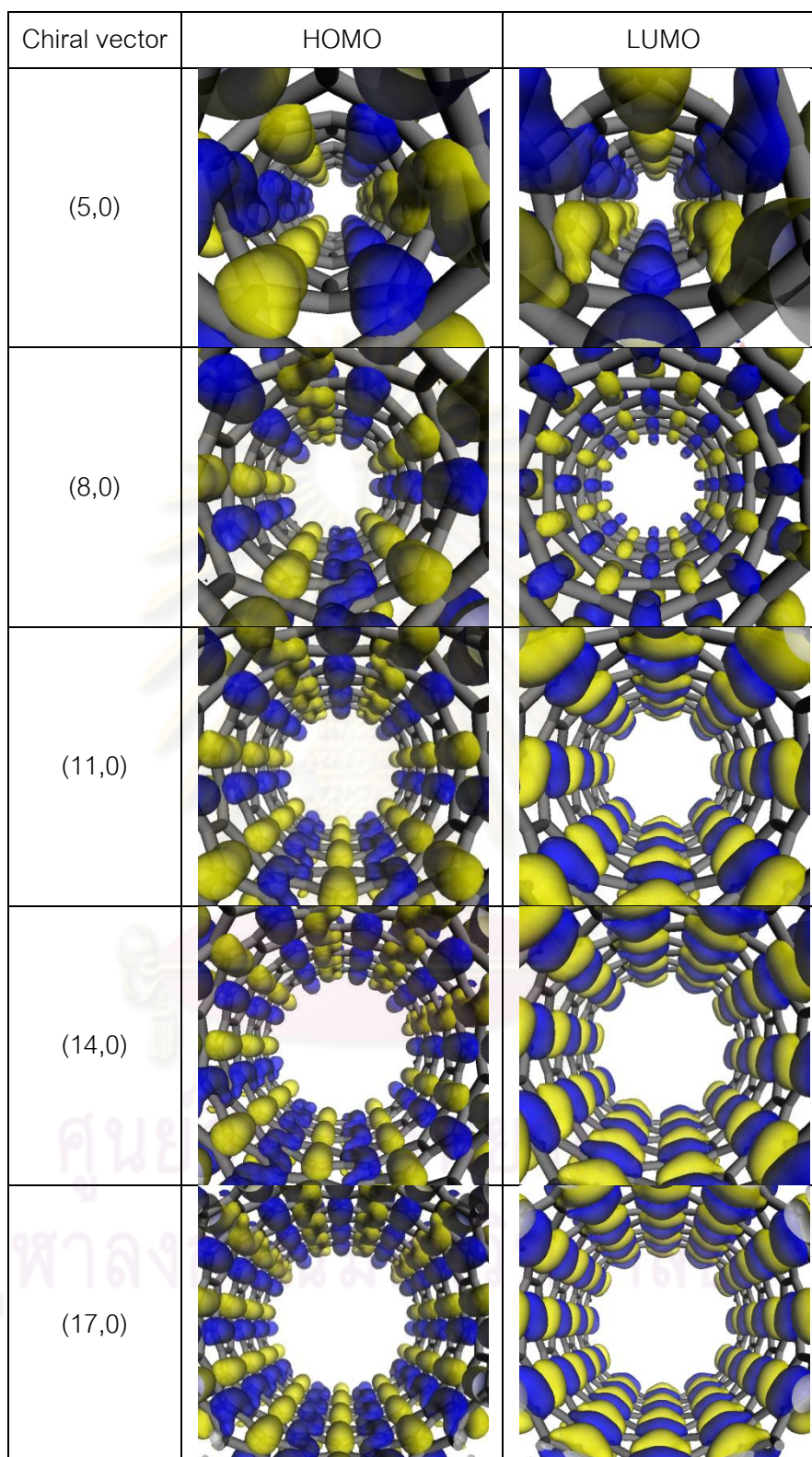


Figure 4.5 HOMO and LUMO of $n=3i+2$ zigzag SWCNTs

4.2 Effect of B-N Doping

Two pairs of B-N were doped on SWCNT at various positions and spin states. Their optimized geometries and energies were determined to identify the most favorable B-N doping position and spin multiplicity. Figure 4.6 presents the relative energies of SWCNTs with various doping scheme and spin states and the most stable doping at various B-N distances. The result indicated that the most preference B-N doping of zigzag (8,0) and armchair (5,5) SWCNTs are the position where B-N distance is the smallest (B-N distance = 1.44 Å and 1.46 Å for zigzag and armchair SWCNTs, respectively). In addition, the substitution of N to the distance longer than one bond from B requires 28.1-42.2 and 25.3-44.7 kcal/mol/B-N pair for B-N doped zigzag (8,0) and armchair (5,5), respectively. This agrees with the suggestion on the bond stability in which $[B-N > C-C > C-N > C-B]^{52}$. Therefore, the most stable structure would require the maximum number of B-N and C-C bonds. Having B next to N maximizes B-N and C-C bonds. Structures with singlet spin has the lowest energy with close shell state. The triplet and quintet of B-N doped zigzag (8,0) SWCNT are 2.7-8.7 and 14.1-22.3 kcal/mole/B-N pair and of armchair (5,5) are, 2.4-6.7 and 10.74-22.9 kcal/mole/B-N pair higher in energy. For higher spin state such as triplet and quintet, the dominant spin densities does not occur on B or N (less than 0.09 electron) as show in tables 4.2 and 4.3 but it were presented on carbon atom near dopant. However, relative energies for all electron spin states and all type of SWCNTs structures increase in the same manner with B-N distance as shown in Figure 4.6.

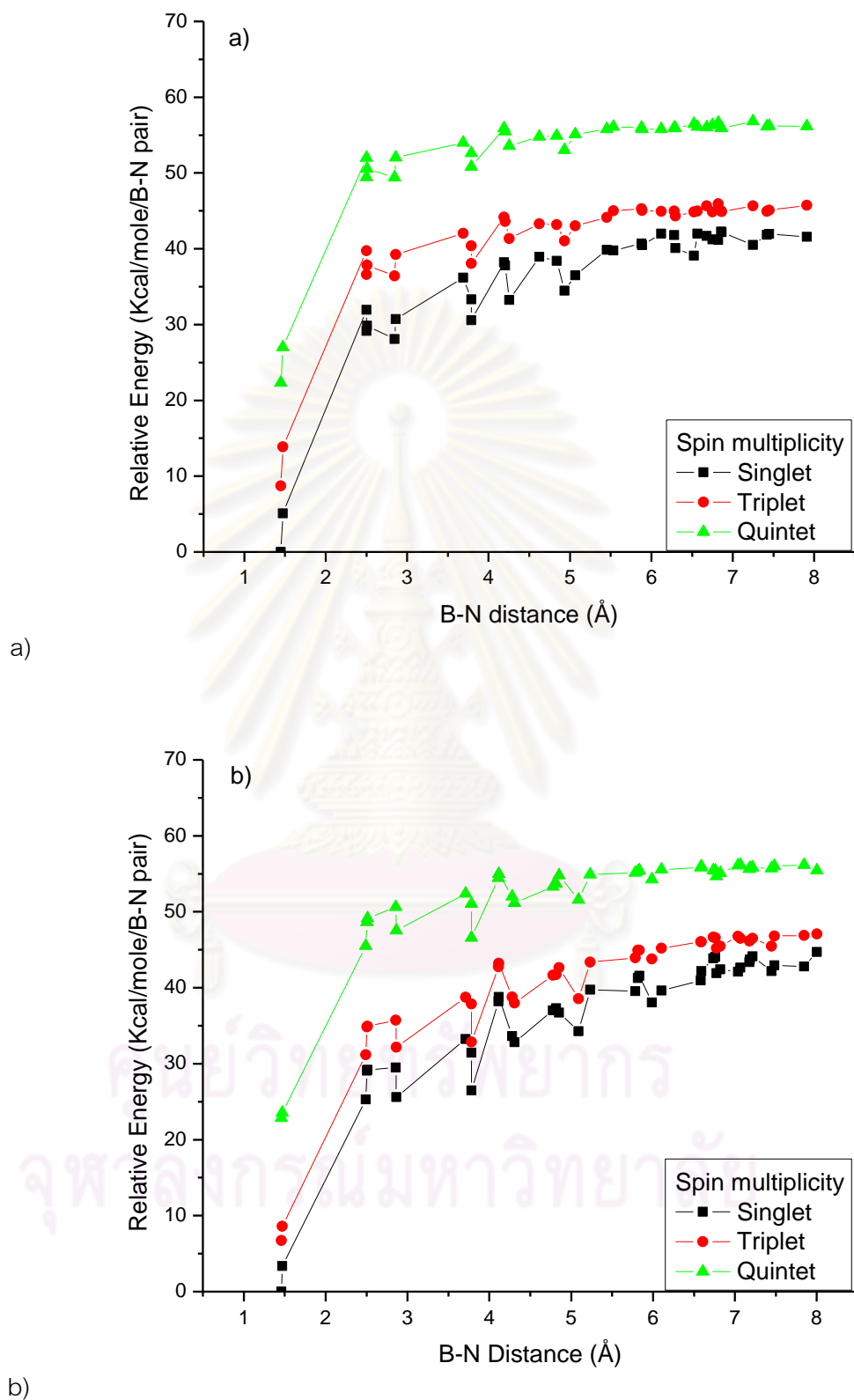


Figure 4.6 Relative energies for the B-N doping as a function of B-N distance of B-N doped a) zigzag (8,0) and b) armchair (5,5) SWCNTs.

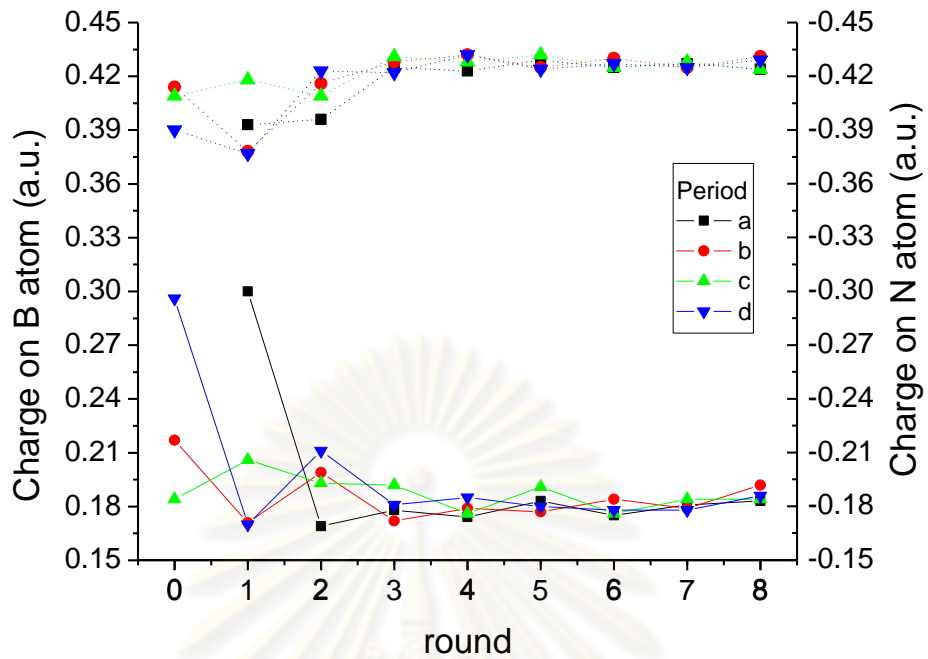
Table 4.2 Spin densities on boron atom and nitrogen atom of zigzag (8,0) SWCNTs

Position of Doping		Triplet spin		Quintet spin	
Round	Period	B atom	N atom	B atom	N atom
1	a	0.033	0.003	0.041	0.011
2	a	0.029	0.016	0.026	0.029
3	a	0.042	0.023	0.041	0.029
4	a	0.037	0.015	0.067	0.052
5	a	0.033	0.021	0.073	0.063
6	a	0.040	0.016	0.077	0.056
7	a	0.041	0.017	0.073	0.056
8	a	0.047	0.019	0.082	0.054
0	b	0.036	0.012	0.064	0.020
1	b	0.043	0.017	0.076	0.037
2	b	0.043	0.020	0.075	0.030
3	b	0.035	0.025	0.063	0.067
4	b	0.038	0.018	0.068	0.054
5	b	0.044	0.019	0.078	0.055
6	b	0.037	0.019	0.073	0.059
7	b	0.039	0.014	0.073	0.051
8	b	0.031	0.018	0.071	0.065
0	c	0.036	0.025	0.066	0.044
1	c	0.039	0.015	0.066	0.032
2	c	0.038	0.021	0.069	0.057
3	c	0.034	0.025	0.038	0.060
4	c	0.036	0.015	0.067	0.050
5	c	0.027	0.019	0.058	0.061
6	c	0.038	0.016	0.075	0.056
7	c	0.040	0.016	0.072	0.055
8	c	0.046	0.019	0.081	0.054
0	d	0.013	0.025	0.020	0.043
1	d	0.035	0.009	0.033	0.029
2	d	0.025	0.012	0.028	0.031
3	d	0.033	0.022	0.033	0.060
4	d	0.034	0.016	0.065	0.051
5	d	0.042	0.018	0.076	0.055
6	d	0.040	0.019	0.077	0.058
7	d	0.040	0.014	0.074	0.051
8	d	0.033	0.017	0.077	0.063

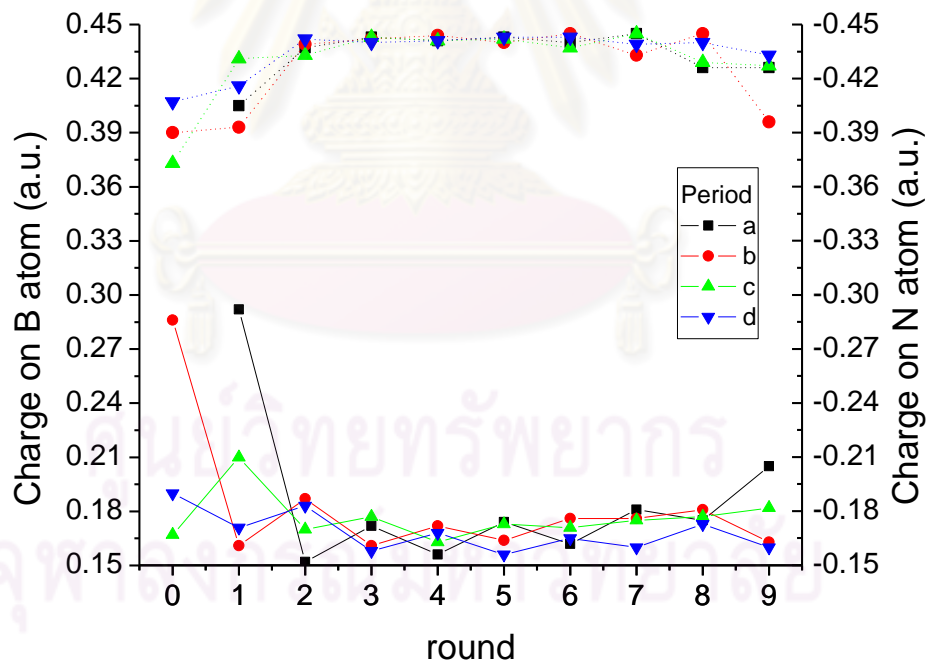
Table 4.3 Spin densities on boron atom and nitrogen atom of armchair (5,5) SWCNTs

Position of Doping		Triplet spin		Quintet spin	
Round	Period	B atom	N atom	B atom	N atom
1	a	0.013	0.013	0.035	0.035
2	a	0.028	0.029	0.055	0.087
3	a	0.024	0.026	0.064	0.074
4	a	0.034	0.045	0.068	0.088
5	a	0.031	0.037	0.072	0.089
6	a	0.034	0.042	0.07	0.085
7	a	0.019	0.021	0.067	0.089
8	a	0.028	0.035	0.063	0.073
9	a	0.014	0.015	0.031	0.052
0	b	0.014	0.014	0.032	0.041
1	b	0.013	0.026	0.044	0.067
2	b	0.019	0.02	0.055	0.062
3	b	0.023	0.039	0.065	0.087
4	b	0.03	0.035	0.07	0.085
5	b	0.029	0.036	0.07	0.087
6	b	0.032	0.041	0.07	0.09
7	b	0.029	0.029	0.068	0.079
8	b	0.019	0.019	0.061	0.087
9	b	0.018	0.008	0.046	0.051
0	c	0.014	0.019	0.04	0.053
1	c	0.015	0.017	0.041	0.045
2	c	0.017	0.035	0.055	0.08
3	c	0.025	0.029	0.065	0.077
4	c	0.026	0.038	0.068	0.087
5	c	0.031	0.038	0.07	0.087
6	c	0.029	0.033	0.069	0.084
7	c	0.031	0.041	0.068	0.09
8	c	0.025	0.023	0.061	0.069
9	c	0.019	0.02	0.059	0.079
0	d	0.021	0.018	0.055	0.065
1	d	0.026	0.024	0.048	0.073
2	d	0.018	0.018	0.049	0.054
3	d	0.031	0.043	0.064	0.086
4	d	0.028	0.032	0.068	0.083
5	d	0.033	0.043	0.068	0.085
6	d	0.032	0.039	0.07	0.088
7	d	0.029	0.039	0.066	0.081
8	d	0.023	0.036	0.066	0.087
9	d	0.022	0.03	0.057	0.069

Figure 4.7 shows Mulliken charges on boron and nitrogen atom in doped zigzag (8,0) and armchair (5,5) SWCNTs, as the function of round and period vector. Boron atom possesses positive charge with values between 0.17 to 0.30 for zigzag and 0.15 to 0.29 for armchair. While nitrogen atom possesses negative charge with values between -0.38 to -0.43 for zigzag and -0.37 to 0.45 for armchair depending on doping position. When the B-N atom is bonded such as at 1a and 0d for zigzag and at 1a and 0b for armchair, charge on B and N become more positive. The oscillation on the value of charges was observed between odd and even number of round vectors for both structures. The similar behavior could also be noticed in case of stabilities of doped SWCNT as seen in Figure 4.6. The oscillation has some characteristic which depends on the symmetry of doping position. However, one must separate cases for odd and even round vectors as done in Figure 4.8. The linear relation between relative stabilities of structures with odd and even round vectors and 1/B-N distance of doped SWCNT was observed when plotting according to period vectors. Positions a1 and d0 are excluded from the plot; since charges that bear on boron and nitrogen atoms in 1a and 0d position are too different for other positions. The square correlation coefficients of linear relation (R^2) from the plots between 1/B-N distances and relative energies of around 0.963 to 0.998 indicates the successful of the fitting of the results to linear equations. This linear relation suggests the importance of the columbic interactions to stabilities of B-N doped SWCNT. The grouping according to period vectors implies the similarity of doped SWCNT with same period vectors and the distinction between those with different period vectors. From Figure 4.7, it could be observed that B and N substituted at the same period vector have similar charge distributions. SWCNTs with same period vector have similar environment and thus similar charge distribution. The different in the nature of SWCNTs at different period vectors could then be explained by the different environment around substituted atoms. However, the odd-even alternation is probably an effect of the distinct electronic structures between SWCNTs substituted at odd and even positions of round vectors.



a)



b)

Figure 4.7 Charge on doped atom in a) zigzag (8,0) and b) armchair (5,5) SWCNTs as functions of position of doping , In the inset solid line represent charge on boron atom and dash line represent charge on nitrogen atom.

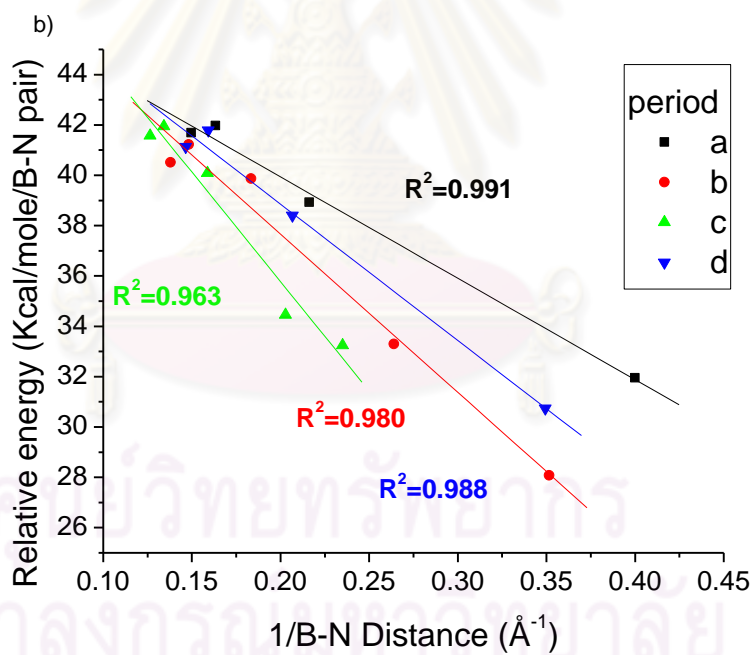
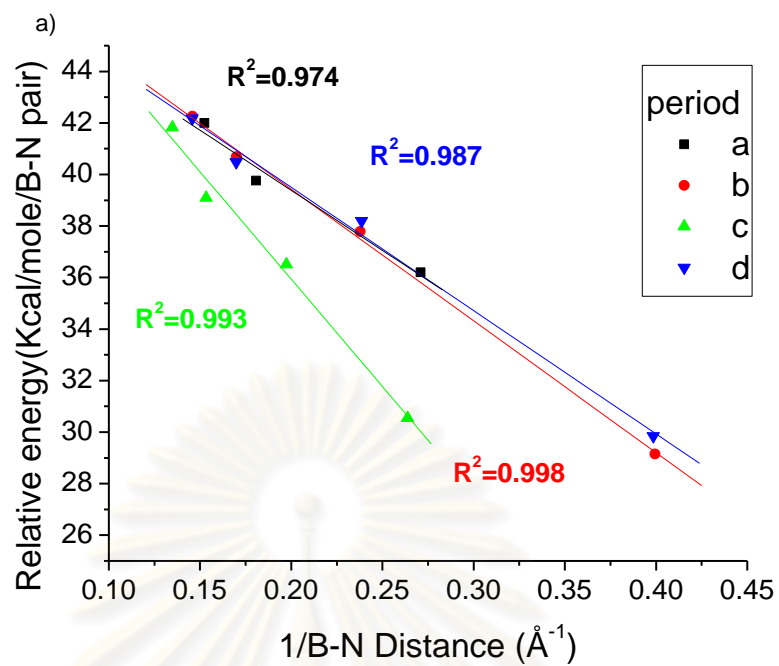


Figure 4.8 Correlation between relative energies and B-N distance reciprocal consideration by symmetry of doping a) odd number and b) even number on round direction of B-N doping for zigzag SWCNT

The effect of B-N doping upon electronic band structures of SWCNTs were investigated. The example of calculated undoped and B-N doped zigzag (8,0) and armchair (5,5) SWCNTs band structure are shown in Figure 4.9. The band gap energy, E_g , which calculated from differences between valence and conduction band energies as a function of B-N doping positions was shown in Figure 4.10. The result indicates that B-N doping on SWCNTs decreases the band gap energy of undoped zigzag (8,0) SWCNT from 0.606 eV to 0.183-0.571 eV depending on doping positions, Figure 4.9a. Similarly, the band gap energy of armchair (5,5) SWCNT reduces from 0.448 to 0.133-0.427 eV depending on doping positions, Figure 4.10b. This observation is in agreement with experiment¹⁵ that synthesized B-N doped SWCNTs by arc discharge method and found that B-N doping effect leads to reduce E_g of SWCNTs. Considering the substitution on the period direction of zigzag (8,0) SWCNT, it was found that dependencies of energies band gap on round vectors are quite similar between B-N substitutions on period a and c and those between period b and d. By closely analyzing B-N doped zigzag (8,0) SWCNT, the doping at period a and c has very similar environment and likewise for that at period b and d. In addition, there is a pattern of maxima and minima on Figure 4.10a. Substitutions on period a, b, c, and d show maximum points of E_g at positions 0, 2, 5, and 8 of round vectors and the minimum points of E_g at positions 1, 4, and 6 or 7 of round vectors. Whereas, positions of doping on period direction of For armchair (5,5), the similarity between patterns of E_g according to period vectors was not found, Figure 4.10b. However, the maximum and minimum of E_g upon round vectors were observed for B-N doped armchair (5,5) SWCNT. The observed maximum points of E_g are on 1a, 7a, 2b, 4b, 9b, 1c, 3c, 5c, 8c, 0d, 6d, and 8d B-N substitutions while the minimum points of E_g are on 3a, 6a, 9a, 0b, 3b, 5b, 8b, 0c, 2c, 4c, 6c, 9c, 5d, 7d, and 9d B-N substitutions. The patterns for E_g are less pronounced than those of stabilities and charges. Again, we expected that B-N substitutions generated different electronic structures. While substitutions in period direction vary external potential which then alters stability, charge distribution, and band gap energy of SWCNT, substitutions along round direction cause the change in electronic structure of SWCNT.

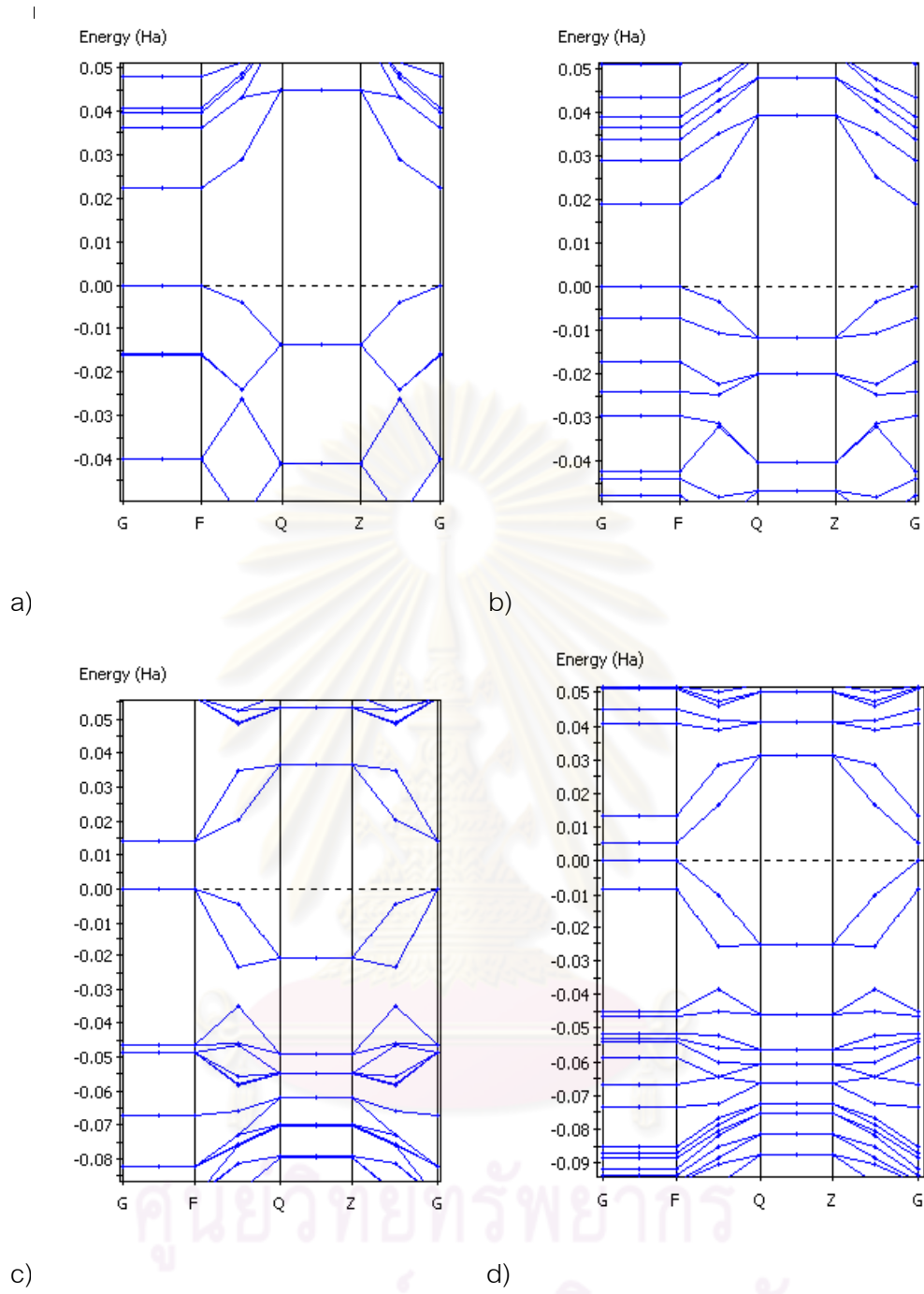


Figure 4.9 Calculated band structure of a) undoped zigzag (8,0) SWCNT b) B-N doped zigzag (8,0) SWCNT at 1a position of doping c) undoped armchair (5,5) SWCNT and d) B-N doped armchair (5,5) SWCNT at 0b position of doping.

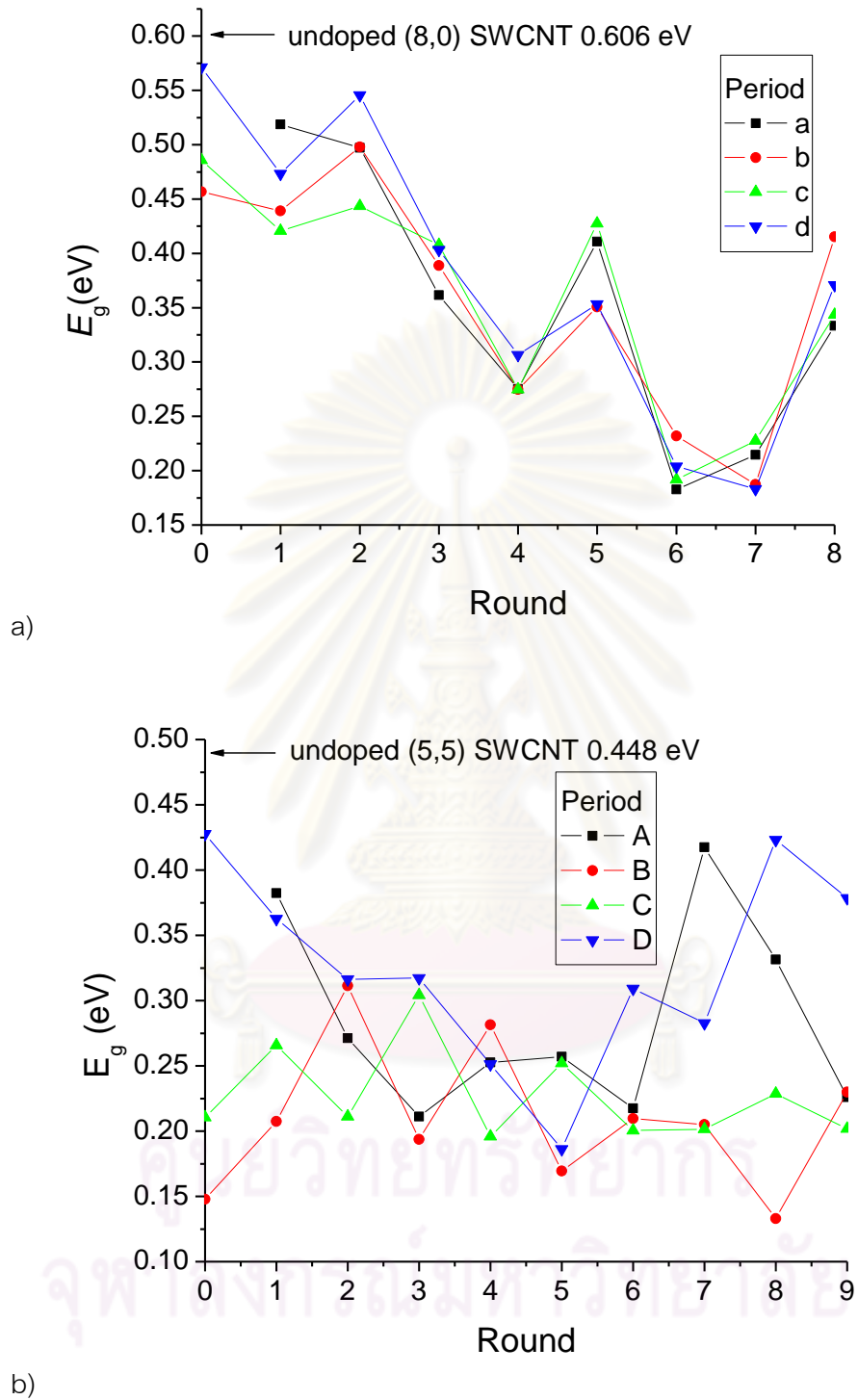


Figure 4.10 Band gap energy (E_g) of undoped and B-N doped a) zigzag (8,0) b) armchair (5,5) SWCNT as a function of doping position

3.2 Effect of External Pressure

To investigate mechanical properties of SWCNTs, stress was applied to undoped and B-N doped zigzag (8,0), and undoped and B-N doped armchair (5,5) SWCNTs along tube axis (c-direction), see Table 3.1. Geometries of structures shown in Table 3.1 were optimized and their energies were determined. Plots of energies of undoped and B-N doped zigzag (8,0) and undoped and B-N doped armchair (5,5) relative to their unstress structures with the stress ratio (ε) were made and displayed in figure 4.11. All structures have similar curvature, in exception of B-N (8,0) which has slightly larger curvature. The curvature of the plot in Figure 4.11 is related to Young's modulus which can be calculated according to

$$Y = \frac{1}{V_0} \left. \frac{\partial^2 E}{\partial \varepsilon^2} \right|_{\varepsilon=0} \quad (4.1)$$

where V_0 is the equilibrium volume, E is the total energy of system and ε is the strain ratio along the tube axis. Young's modulus values of undoped and B-N doped (8,0) and (5,5) SWCNTs were given in table 4.4.

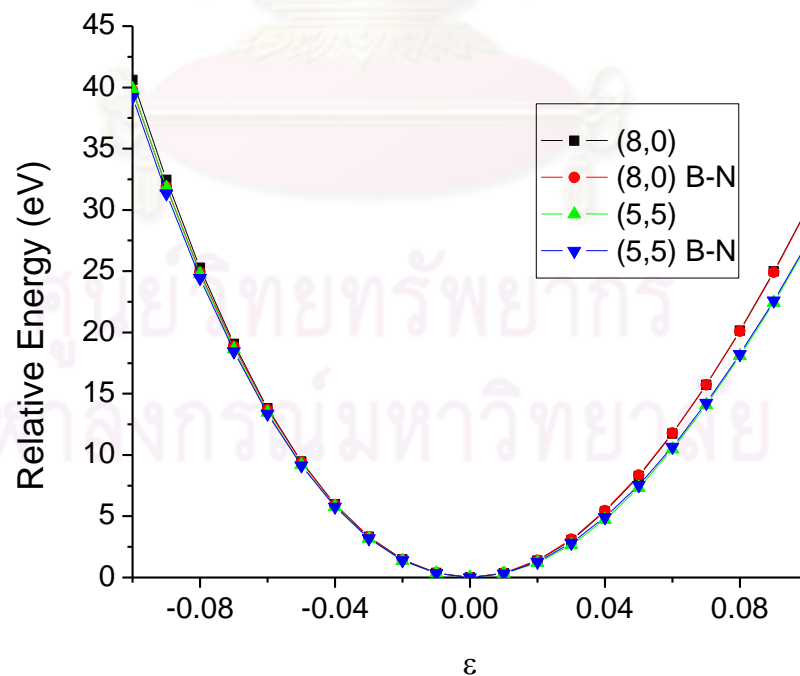


Figure 4.11 Relative energy of undoped and B-N doped zigzag (8,0) and armchair (5,5) SWCNT as a function of strain ratio

Table 4.4 Young's modulus value obtained from DFT comparing with other calculation and experimental works.

SWCNT	Young's Modulus (TPa)				
	This work	HF ⁹	Finite Element ³¹	TEM ³²	AFM ³³
(8,0)	1.082	1.306	0.910	1.25	1.0
(8,0) B-N doped	1.069	-	-		
(5,5)	1.101	1.293	0.919		
(5,5) B-N doped	1.091	-	-		

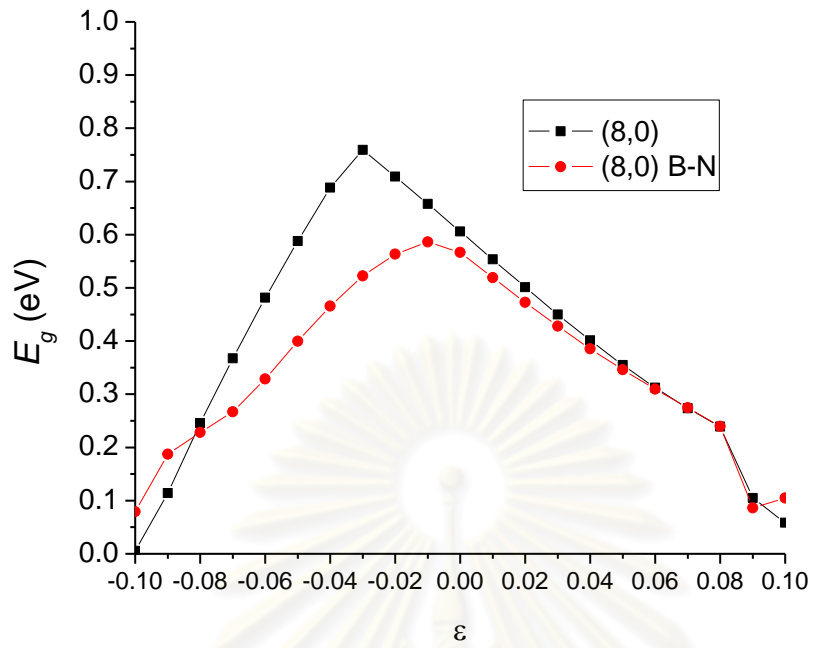
Values of Young's modulus obtained from this work are 1.082 and 1.091 TPa for undoped (8,0) and (5,5) SWCNTs, the values agree well with those obtained from previous calculations and experiments. However, both TEM and AFM were performed on mixtures of SWCNTs and their values are varied. Since values of Young's modulus of zigzag and armchair SWCNTs are very similar, experimental values can still be used to represent SWCNTs. For B-N doped SWCNTs, Young's modulus values are slightly smaller than the undoped SWCNTs, i.e. 1.069 and 1.091 TPa for B-N doped zigzag (8,0) and armchair (5,0), respectively. Thus, B-N doping almost has no effect on mechanical properties of SWCNTs.

The effect of stress on the electronic band gap of undoped and B-N doped SWCNTs were investigated and the result was displayed in Figure 4.11 which showed the change of E_g with stress ratio (ϵ). From the graph, It is observed that the E_g of undoped zigzag (8,0) SWCNT decreases from 0.6 eV to nearly 0 eV when applying stress, $\epsilon = 0.0$ to 0.1. However, when applying stress $\epsilon = -0.03$ E_g reaches maximum with the value of 0.8 eV and it reduces afterward to 0 eV at $\epsilon = -0.1$. The similar behavior is observed for B-N doped zigzag (8,0) SWCNT, i.e. decreases to nearly 0 eV when $\epsilon = 0.0$ to -0.1 and = 0.0 to 0.1. In this case, the maximum is at $\epsilon = 0.0$. For undoped and B-N doped armchair (5,5) SWCNT, E_g does not monotonically decreases like that of the zigzag but it rather oscillates with ϵ . Moreover, the undoped and B-N doped armchair do not share the same behavior. For both cases, E_g can be reduces to the value close to

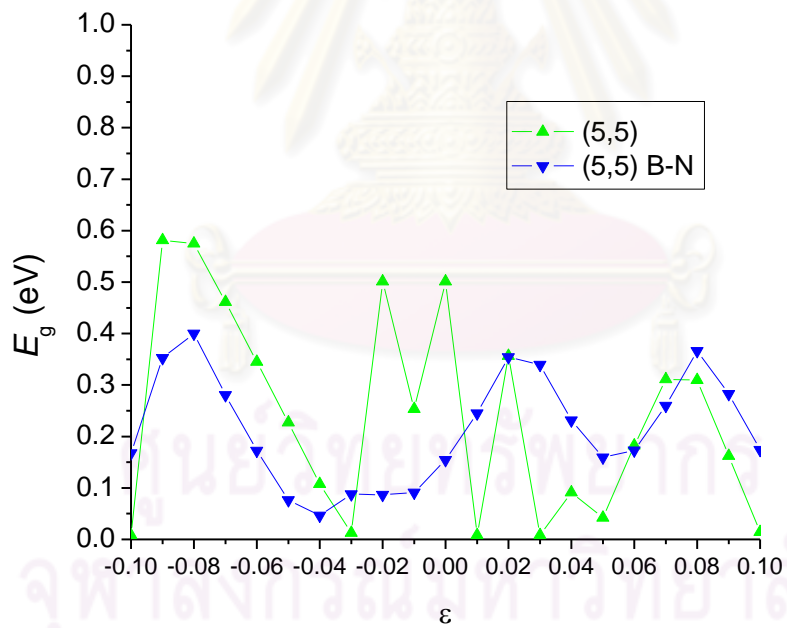
0 eV. For undoped armchair (5,5) SWCNT, E_g is the highest (0.58 eV) at $\varepsilon = -0.09$. For B-N doped armchair (5,5) SWCNT, appear the maximum point of E_g is the highest (0.40 eV) at $\varepsilon = -0.08$. The stress or external pressure while has almost no effect on mechanical property such as Young's modulus, it has a drastic effect on the electronic band energy of undoped and B-N doped SWCNTs.



ศูนย์วิทยทรัพยากร
จุฬาลงกรณ์มหาวิทยาลัย



a)



b)

Figure 4.11 Band gap energy (E_g) of undoped and B-N doped a) zigzag (8,0) and b) armchair (5,5) SWCNT as a function of strain ratio

CHAPTER V

CONCLUSION

Effects of tube diameter, B-N doping and external pressure (stress) on electronic band structures of zigzag and armchair SWCNTs with various tube diameter (D) were investigated using density functional PBE with DND or DNP basis set. The results revealed linear tendency of strain energy with $1/D^2$ when comparing with graphene sheet for both zigzag and armchair SWCNTs. The linear relationship was observed between band gap energies and $1/D$ of $(3i+1)$ and $(3i+2)$ zigzag SWCNT and between band gap energies of and $1/D^2$ armchair SWCNT. For very small tube diameter (smaller than 5 Å), most SWCNTs are metal or semimetal. The maxima of band gap energies of SWCNTs was observed when the tube diameters are in the range of 5-7 Å. The $(3i+1)$ and $(3i+2)$ zigzag SWCNTs have the maximum band gap energies around 0.9 eV and at tube diameter of 9 Å and their band gap energies are converged to 0 eV for very large diameter while $3i$ zigzag and armchair SWCNTs have a very small to zero band gap that are being metal for all range of tube diameter. The distinction in electronic properties of very small diameter SWCNTs probably are a result of the change in atomic hybridization of C atom from sp^2 to sp^3 as predicted from bond lengths and bond angles of SWCNTs. This change in atomic hybridization also affects the electronic structures of SWCNTs.

Various B-N doping were performed for zigzag (8,0) and armchair (5,5) SWCNTs. Favorable B-N doping positions and spin states for both zigzag and armchair SWCNTs were identified by comparing their energies. The results indicated that the most favorable electron spin state is closed shell singlet and the most stable doping position is that with the B-N closest distance. From plots of stabilities of armchair and zigzag SWCNTs and B-N distances, the oscillation pattern is observed. Stabilities of SWCNTs show linear relationship $1/B-N$ distance suggesting that stabilities of B-N doped SWCNTs are governed by columbic interaction between positively charged boron and negatively charged nitrogen atoms. Band gap energies of B-N doped

SWCNTs depend on the position of doping. There are positions on round vectors which maxima and minima band gap energies were observed. Although there exhibits patterns, no explanation can be given, except these patterns are the result of variations in electronic structures. These variations are more dependent on round than period vectors. For zigzag SWCNTs, patterns can be grouped according to period vectors, i.e. a-d and b-c. This is not the case for armchair SWCNTs. The grouping is the result of similar environments of the period vectors.

By applying external pressure to undoped and doped armchair (5,5) and zigzag (8,0) SWCNTs, Young's modulus value could be calculated. It was found that B-N doping has almost no effect on Young's modulus. Also the result indicates that undoped and B-N doped armchair (5,5) are mechanically stronger than zigzag (8,0) SWCNTs. However, undoped and B-N doped SWCNTs still have Young's modulus value in the order of TPa. Thus, they are considered to be one of the stiffest material yet discovered. In addition, it was observed that electronic band gaps of these materials changed when applying external pressure along the tube axis. For zigzag SWCNTs, external pressure with both positive and negative strain ratio would reduce its band gap energy and the material could turn from semiconductor to metallic. For armchair SWCNTs, the change in the band gap energy is also evident, however, with no regular patterns like in the case of zigzag SWCNTs. In additions, the patterns for band gap energy when applying external pressure are dissimilar for undoped and B-N doped armchair SWCNTs. Thus, cautions must be made when bringing SWCNTs to subject to external pressure.

Tube diameters, external pressure and B-N doping could change electronic properties of armchair and zigzag SWCNTs. From this study, we could summarize the changes and it could be used as the guide for selection of appropriate SWCNTs which could be useful for application in electronic devices.

REFERENCES

- [1] Boehm, H. P. The first observation of carbon nanotubes. *Carbon* 35 (1997) : 581.
- [2] Monthieux, M.; and Kuznetsov, V. L. Who should be given the credit for the discovery of carbon nanotubes? *Carbon* 44 (2006) : 1621.
- [3] Oberlin, A.; Endo, M.; and Koyama, T. Filamentous growth of carbon through benzene decomposition. *Journal of Crystal Growth* 32 (1976) : 335.
- [4] Abrahamson, J.; Wilse, P. G.; and Rhoades, B. L. Structure of carbon fibers found on carbon arc anodes. *Carbon* 37 (1999) : 1873.
- [5] Iijima, S. Helical microtubules of graphitic carbon. *Nature* 354 (1991) : 56.
- [6] Hamada, N.; Sawada, S. i.; and Oshiyama, A. New one-dimensional conductors: Graphitic microtubules. *Physical Review Letters* 68 (1992) : 1579.
- [7] Saito, R.; Fujita, M.; Dresselhaus, G.; and Dresselhaus, M. S. Electronic structure of chiral graphene tubules. *Applied Physics Letters* 60 (1992) : 2204.
- [8] Dresselhaus, M. S.; Dresselhaus, G.; and Saito, R. Physics of carbon nanotubes. *Carbon* 33 (1995) : 883.
- [9] Peng, Y. J.; Zhang, L. Y.; Jin, Q. H.; Li, B. H.; and Ding, D. T. Ab initio studies of elastic properties and electronic structures of C and BN nanotubes. *Physica E- Low-Dimensional Systems & Nanostructures* 33 (2006) : 155.
- [10] Barone, V.; and Scuseria, G. E. Theoretical study of the electronic properties of narrow single-walled carbon nanotubes: Beyond the local density approximation. *Journal of Chemical Physics* 121 (2004) : 10376.
- [11] Blase, X.; Benedict, L. X.; Shirley, E. L.; and Louie, S. G. Hybridization effects and metallicity in small radius carbon nanotubes. *Physical Review Letters* 72 (1994) : 1878.
- [12] Liu, H. J.; Li, Z. M.; Liang, Q.; Tang, Z. K.; and Chan, C. T. Carbon nanotubes-zeolite complex: A Li-intercalated compound with high storage capacity. *Applied Physics Letters* 84 (2004) : 2649.
- [13] Zhao, X.; Liu, Y.; Inoue, S.; Suzuki, T.; Jones, R. O.; and Ando, Y. Smallest Carbon Nanotube Is 3 Å ring; in Diameter. *Physical Review Letters* 92 (2004) : 125502.

- [14]Li, Z. M.; Tang, Z. K.; et al. Polarized absorption spectra of single-walled 4 angstrom carbon nanotubes aligned in channels of an AlPO₄-5 single crystal. *Physical Review Letters* 87 (2001) : 12.
- [15]Wang, B.; Ma, Y. F.; Wu, Y. P.; Li, N.; Huang, Y.; and Chen, Y. S. Direct and large scale electric arc discharge synthesis of boron and nitrogen doped single-walled carbon nanotubes and their electronic properties. *Carbon* 47 (2009) : 2112.
- [16]Stephan, O.; Ajayan, P. M.; et al. Doping graphitic and carbon nanotube structures with boron and nitrogen. *Science* 266 (1994) : 1683.
- [17]Gai, P. L.; Stephan, O.; et al. Structural systematics in boron-doped single wall carbon nanotubes. *Journal of Materials Chemistry* 14 (2004) : 669.
- [18]Glerup, M.; Steinmetz, J.; et al. Synthesis of N-doped SWNT using the arc-discharge procedure. *Chemical Physics Letters* 387 (2004) : 193.
- [19]Redlich, P.; Loeffler, J.; Ajayan, P. M.; Bill, J.; Aldinger, F.; Ruhle, M., B-C-N nanotubes and boron doping of carbon nanotubes. *Chemical Physics Letters* 260 (1996) : 465.
- [20]Terrones, M.; Hsu, W. K.; et al Metal particle catalysed production of nanoscale BN structures. *Chemical Physics Letters* 259 (1996) : 568.
- [21]Terrones, M.; Grobert, N.; et al. Controlled production of aligned-nanotube bundles. *Nature* 388 (1997) : 52.
- [22]Terrones, M.; Hsu, W. K.; Ramos, S.; Castillo, R.; Terrones, H., The role of boron nitride in graphite plasma arcs. *Fullerene Science and Technology*. 6 (1998) : 787.
- [23]Terrones, M.; Redlich, P.; et al. Carbon nitride nanocomposites: Formation of aligned C_xN_y nanofibers. *Advanced Materials* 11 (1999) : 655.
- [24]Buonocore, F., Doping effects on metallic and semiconductor single-wall carbon nanotubes. *Philosophical Magazine* 87 (2007) : 1097.
- [25]Zhang, Y. M.; Zhang, D. J.; and Liu, C. B. Novel chemical sensor for cyanides: Boron-doped carbon nanotubes. *Journal of Physical Chemistry B* 110 (2006) : 4671.

- [26]Peng, S.; and Cho, K. J. Ab initio study of doped carbon nanotube sensors. *Nano Letters* 3 (2003) : 513.
- [27]Wei, J.; Hu, H.; Zeng, H.; Zhou, Z.; Yang, W.; and Peng, P. Effects of nitrogen substitutional doping on the electronic transport of carbon nanotube. *Physica E-Low-Dimensional Systems & Nanostructures* 40 (2008) : 462.
- [28]Owens, F. J. Boron and nitrogen doped single walled carbon nanotubes as possible dilute magnetic semiconductors. *Nanoscale Research Letters* 2 (2007) : 447.
- [29]Wang, W. L.; Bai, X. D.; et al. Direct Synthesis of B-C-N Single-Walled Nanotubes by Bias-Assisted Hot Filament Chemical Vapor Deposition. *Journal of the American Chemical Society* 128 (2006) : 6530.
- [30]Moradian, R.; and Azadi, S. Boron and nitrogen-doped single-walled carbon nanotube. *Physica E-Low-Dimensional Systems & Nanostructures* 35 (2006) : 157.
- [31]Meo, M.; and Rossi, M. Prediction of Young's modulus of single wall carbon nanotubes by molecular-mechanics based finite element modelling. *Composites Science and Technology* 66 (2006) : 1597.
- [32]Krishnan, A.; Dujardin, E.; Ebbesen, T. W.; Yianilos, P. N.; and Treacy, M. M. J. Young's modulus of single-walled nanotubes. *Physical Review B* 58 (1998) : 14013.
- [33]Wong, E. W.; Sheehan, P. E.; and Lieber, C. M. Nanobeam mechanics: Elasticity, strength, and toughness of nanorods and nanotubes. *Science* 277 (1997) : 1971.
- [34]Sreekala, S.; Peng, X. H.; Ajayan, P. M.; and Nayak, S. K. Effect of strain on the band gap and effective mass of zigzag single-wall carbon nanotubes: First-principles density-functional calculations. *Physical Review B* 77 (2008) : 15.
- [35]Zhang, J. M.; Liang, R. L.; and Xu, K. W. Effect of uniaxial strain on the band gap of zigzag carbon nanotubes. *Physica B-Condensed Matter* 405 (2010) : 1329.
- [36]Ito, T.; Nishidate, K.; Baba, M.; and Hasegawa, M. First principles calculations for electronic band structure of single-walled carbon nanotube under uniaxial strain, *Surface Science* 514 (2002) : 222.
- [37]Horodecki, R. De broglie wave and its dual wave. *Physics Letters* 514 (1981) : 95.

- [38]Roothaan, C. C. J. New developments in molecular orbital theory. *Reviews of Modern Physics* 23 (1951) : 69.
- [39]Hall, G. G. The molecular orbital theory of chemical valency. VIII. A method of calculating ionization potentials. *Proceedings of the Royal Society of London. Series A. Mathematical and Physical Sciences* 205 (1951) : 541.
- [40]Hohenberg, P.; and Kohn, W. Inhomogeneous Electron Gas. *Physical Review* 136 (1964) : 864.
- [41]Kohn, W.; and Sham, L. J. Self-Consistent Equations Including Exchange and Correlation Effects. *Physical Review* 140 (1965) : 1133.
- [42]Slater, J. C. Statistical exchange-correlation in the self-consistent field. *Advanced quantum chemistry* 6 (1972) : 1.
- [43]Vosko, S. J. W., L.; and Nusair, M. Accurate spin-dependent electron liquid correlation energies for local spin density calculations: A critical analysis. *Canadian Journal of Physics* 58 (1980) : 1200.
- [44]Perdew, J. P.; Burke, K.; and Ernzerhof, M. Generalized gradient approximation made simple. *Physical Review Letters* 77 (1996) : 3865.
- [45]Staroverov, V. N.; Scuseria, G. E.; Tao, J.; and Perdew, J. P. Tests of a ladder of density functionals for bulk solids and surfaces. *Physical Review B* 69 (2004) : 75.
- [46]Delley, B. An all-electron numerical method for solving the local density functional for polyatomic molecules. *The Journal of Chemical Physics* 92 (1990) : 508.
- [47]Delley, B. Analytic energy derivatives in the numerical local-density-functional approach. *The Journal of Chemical Physics* 94 (1991) : 7245.
- [48]Delley, B. From molecules to solids with the DMol³ approach. *Journal of Chemical Physics* 113 (2000) : 7756.
- [49]Monkhorst, H. J.; and Pack, J. D. Special points for Brillouin-zone integrations. *Physical Review B* 13 (1976) : 5188.
- [50]Yang, L.; and Han, J. Electronic structure of deformed carbon nanotubes. *Physical Review Letters* 85 (2000) : 154.

[51]Yang, L.; Anantram, M. P.; Han, J.; and Lu, J. P. Band-gap change of carbon nanotubes: Effect of small uniaxial and torsional strain. *Physical Review B* 60 (1999) : 13874.

[52]Ivanovskaya, V. V.; Zobelli, A.; Stephan, O.; Briddon, P. R.; and Colliex, C. BN Domains Included into Carbon Nanotubes: Role of Interface. *Journal of Physical Chemistry C* 113 (2009) : 16603.



ศูนย์วิทยทรัพยากร
จุฬาลงกรณ์มหาวิทยาลัย

VITAE

NAME: Arthit Vongachariya

DATE AND PLACE OF BIRTH: 20 July 1986 in Bangkok, Thailand

ELEMENTARY SCHOOL:

1992-1998 Sarasas Pithaya School, Bangkok

SECONDARY SCHOOL:

1998-2001 Sarasas Pithaya School, Bangkok

2001-2004 Sarasas Ektra School, Bangkok

UNIVERSITY EDUCATION:

2004-2008 B.Sc. in Department of Chemistry, Faculty of Science, Chulalongkorn University, Bangkok

2008-2010 M. Sc. In Physical Chemistry, Department of Chemistry, Faculty of Science, Chulalongkorn University, Bangkok

SCHOLARSHIPS:

2005-2008 Human Resource Development in Science Project

2007 Young Scientist and Technologist Programme

2008-2010 ADB, National Center of Excellence for Petroleum, Petrochemicals, and Advanced Materials, NCE-PPAM

2009 Japan-East Asia Network of Exchange for Students and Youths (JENESYS) Fellowship, Kyoto University

2009 Japan-East Asia Network of Exchange for Students and Youths (JENESYS) Fellowship, Institute for Molecular Science (IMS)

2010 The 90th of Chulalongkorn University Fund (Ratchadaphiseksomphot Endowment Fund)